

SECRET
(When Filled In)

Approved For Release 2002/09/04 : CIA-RDP67B00820R000300110031-7		CONTRACT NO. BB 425		TASK NO. 4			
CONTRACT INSPECTION REPORT							
TO: ENGINEERING SECTION/CB/PD/OL		DATE 29 June 1964					
BB 425 TOP TAP		INSPECTION REPORT NO. (If final, so state) 8					
		ESTIMATED COMPLETION DATE June 1964					
NAME OF CONTRACTOR Itek Corporation, Mass.							
TYPE OF COMMODITY OR SERVICE Image Enhancement Viewer							
CONTRACT INSPECTOR R. Sw 7/8/64							
THE CONTRACTOR IS ON SCHEDULE <input type="checkbox"/> YES <input checked="" type="checkbox"/> NO			THE CONTRACTOR WILL PROBABLY REMAIN WITHIN ALLOCATED FUNDS <input type="checkbox"/> YES <input type="checkbox"/> NO				
THE CONTRACTOR WILL COMPLETE TASK WITHIN ALLOTTED TIME <input type="checkbox"/> YES <input type="checkbox"/> NO			ALL PHASES OF THE TECHNICAL PROGRESS ARE SATISFACTORY <input type="checkbox"/> YES <input type="checkbox"/> NO				
HAS AN INTERIM REPORT, FINAL REPORT, PROTOTYPE, OR OTHER END ITEM BEEN RECEIVED FROM THE CONTRACTOR DURING THE PERIOD? <input checked="" type="checkbox"/> YES <input type="checkbox"/> NO (If yes, give details on reverse side.)							
HAS GOVERNMENT-OWNED PROPERTY BEEN DELIVERED TO CONTRACTOR DURING THIS PERIOD? <input type="checkbox"/> YES <input checked="" type="checkbox"/> NO (If yes, indicate items, quantity, and cost on reverse side.)							
OVERALL PERFORMANCE OF CONTRACTOR							
1. <input type="checkbox"/> OUTSTANDING 3. <input type="checkbox"/> EXCELLENT 5. <input checked="" type="checkbox"/> ACCEPTABLE 7. <input type="checkbox"/> UNSATISFACTORY							
2. <input type="checkbox"/> SUPERIOR 4. <input type="checkbox"/> HIGHLY SATISFACTORY 6. <input type="checkbox"/> BARELY ADEQUATE							
IF OVERALL PERFORMANCE OF CONTRACTOR IS UNSATISFACTORY OR BARELY ADEQUATE, INDICATE REASONS ON REVERSE SIDE.							
RECOMMENDED ACTION							
<input checked="" type="checkbox"/> CONTINUE AS PROGRAMMED <input type="checkbox"/> WITHHOLD PAYMENT PENDING SATISFACTORY PERFORMANCE							
<input type="checkbox"/> TERMINATE <input type="checkbox"/> OTHER (Specify)							
IF TERMINATION IS RECOMMENDED OR IF THIS IS A FINAL REPORT, CERTIFY THAT ALL DELIVERABLE ITEMS UNDER THE CONTRACT HAVE BEEN RECEIVED. THESE INCLUDE, WHERE APPLICABLE, THE FOLLOWING:							
ITEM		REC'D	DOES NOT APPLY	ITEM	REC'D	DOES NOT APPLY	
PROTOTYPES		X		MANUALS			
DRAWINGS AND SPECIFICATIONS				FINAL REPORT	see reverse		
PRODUCTION AND/OR OTHER END ITEMS				SPECIAL TOOLING			
DATE OF LAST CONTACT WITH CONTRACTOR 14 May 1964		OTHER GOVERNMENT PROPERTY					
SIGNATURE OF INSPECTOR			DIVISION				
INSPECTOR'S EXTENSION 3308			P&DC				

The Image Enhancement Viewer has been accomplished. The final report is still being edited and hopefully will be received in the near future.

GOVERNMENT

FINAL REPORT

Itek 9043-1

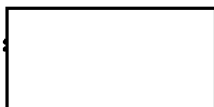
SYSTEMS

23 OCTOBER 1964

A Study of Spatial Filtering Using the Image Enhancement Viewer

25X1A

Authors:



Itek

Itek Corporation

10 Maguire Road Lexington, Massachusetts

SYMBOLS

$F(x)$	Intensity distribution in object space
x	Object coordinate
$F(\omega)$	Amplitude distribution in frequency space
k	Linear frequency
ω	Radian frequency ($2\pi k$) coordinate
$G(\omega)$	Filter characteristic in frequency space
ω_1	Filter cutoff frequency
$H(z)$	Amplitude distribution in image space
z	Image coordinate
T_2	Maximum transmission level
T_1	Minimum transmission level
c	Variance of the Gaussian pulse

CONTENTS

1. Introduction	1
2. Theoretical Study of the Effect of Occluding Filters on an Unsharp (Gaussian) Pulse . . .	2
3. Experimental Filtering of a Nonsharp Edge	15
4. Edge Enhancement Through Exposure Addition	18
5. Application of Spatial Filtering to the Examination of Aerial Photographs	22
6. Application of Spatial Filtering to Mensuration	24

FIGURES

1. Linear, Coherent Optical System Focal Planes of Interest and Defining the Notation and Location of the Fourier Transform Planes	7
2. Intensity Distribution of a Dark- and a Light-Centered Gaussian Spatial Pulse	8
3. Intensity Distribution of a Dark-Centered Gaussian Spatial Pulse With an Occluding Spatial Filter of Radius ω_1 , Showing Some of the Important Pulse and Filter Constants	9
4. Images of Nonsharp Gaussian Pulses of Varying Minimum Transmissive Level, Filtered With Occluding Spatial Filters in a Linear, Coherent Optical System	10
5. Parameters Relating the Linear Frequency, k , the Pulse Variance, c , for Values of $a = 0, 0.25, 0.50, 1.0, 1.5$, and 2.0	14
6. Plots of the Intensity Distribution in the Aerial Image of an Unfiltered and Two Filtered Edges	16
7. Normalized Intensity Distribution of the Image of Two Experimentally Filtered Edges	17
8. Sensitometric Curves for Enhanced Edges on Panatomic-X Film Developed in D-19 for 6 Minutes	20
9. Change of Slope of an Edge With a Varying Ratio of Unfiltered Time to Filtered Time Using the Technique of Exposure Addition	21
10. Four Lens-Film Transfer Functions Using SO-243 Film	23

TABLES

1. Slope of Traced, Enhanced Edges	19
2. Contrast of Traced, Enhanced Edges	19

1. INTRODUCTION

25X1A

The work done under the present phase of the contract consisted of two main parts: first, the modification of the image enhancement viewer and the testing and calibration of this instrument; second, the continuance of research, in certain areas, which had been carried out by [] while working under previous contracts for the viewer.

A description of the modified viewer, along with the methods of testing and calibration, is contained in the operating manual. The viewer was put in working order to the specifications listed in the manual.

The following five research areas were investigated:

1. A nonsharp, Gaussian pulse was theoretically passed through an optical, coherent system. The low frequencies of the pulse were filtered with a high pass occluding filter, and the final images were plotted.
2. A filmed nonsharp edge was experimentally filtered using the viewer, and the image of the edge was traced with a scanning photometer. The results of this trace were curve fitted, normalized, and plotted.
3. Techniques (in this study, mainly exposure addition) for increasing edge contrast and sharpness using the viewer were experimentally examined.
4. The application of various filtering techniques using actual aerial photographs was studied.
5. Finally, the use of occluding spatial filtering as a tool in the area of photographic mensuration was investigated.

From the study of these five areas, a comprehensive view of the capabilities and limitations of the image enhancement viewer and occluding spatial filtering may be obtained.

2. THEORETICAL STUDY OF THE EFFECT OF OCCLUDING FILTERS ON AN UNSHARP (GAUSSIAN) PULSE

A full description of the image enhancement viewer (Fig. 1) and its basic properties may be found in both the operation manual and Itek Technical Report OD-61-6. In operation, the viewer employs coherent illumination, permitting an analysis of the system to treat it as being linear in amplitude.

Since all object films used in the system are immersed in an index matching fluid (see manual) there should be no shift in phase, and the object may be considered solely in terms of amplitude.

In order to obtain a general idea of the effect of occluding filtering on amplitude objects, a generalized case (considered Gaussian for mathematical simplicity) was considered theoretically. This Gaussian pulse is transformed into the frequency plane and there filtered by a circular, centered occluding filter of generalized dimension. The resulting distribution is then again transformed into a filtered image, which has been computed and plotted for the range at representative values.

Considering a nonsharp pulse of Gaussian form (Fig. 2)

$$f_1(x) = T_2 - (T_2 - T_1) \exp(-cx^2)$$

where $f_1(x)$ is the intensity distribution of a dark-centered pulse in the object plane. Its amplitude spectrum in the frequency plane is given by

$$F(\omega) = \int_{-\infty}^{\infty} [f_1(x)]^{\frac{1}{2}} \exp(-i\omega x) dx$$

Then, $[f_1(x)]^{\frac{1}{2}}$ may be rewritten in the following form

$$\begin{aligned} [f_1(x)]^{\frac{1}{2}} &= [T_2 - (T_2 - T_1) \exp(-cx^2)]^{\frac{1}{2}} \\ &= \sqrt{T_2} \left[1 - \left(1 - \frac{T_1}{T_2} \right) \exp(-cx^2) \right]^{\frac{1}{2}} \end{aligned}$$

Expanding, we get

$$\begin{aligned} \left[1 - \left(1 - \frac{T_1}{T_2} \right) \exp(-cx^2) \right]^{\frac{1}{2}} &= 1 - \frac{1}{2} \left(1 - \frac{T_1}{T_2} \right) \exp(-cx^2) - \frac{1}{2 \times 4} \left(1 - \frac{T_1}{T_2} \right)^2 \exp(-2cx^2) \\ &\quad - \frac{1 \times 3}{2 \times 4 \times 6} \left(1 - \frac{T_1}{T_2} \right)^3 \exp(-3cx^2) \\ &\quad - \frac{1 \times 3 \times 5}{2 \times 4 \times 6 \times 8} \left(1 - \frac{T_1}{T_2} \right)^4 \exp(-4cx^2) \\ &\quad - \frac{1 \times 3 \times 5 \times 7}{2 \times 4 \times 6 \times 8 \times 10} \left(1 - \frac{T_1}{T_2} \right)^5 \exp(-5cx^2) - \dots \end{aligned}$$

Letting the binomial coefficients be

$$A(1) = \frac{1}{2}$$

$$A(2) = \frac{1}{2 \times 4}$$

$$A(3) = \frac{1 \times 3}{2 \times 4 \times 6}$$

$$A(4) = \frac{1 \times 3 \times 5}{2 \times 4 \times 6 \times 8}$$

$$A(5) = \frac{1 \times 3 \times 5 \times 7}{2 \times 4 \times 6 \times 8 \times 10}$$

$$\vdots$$

$$\text{Then } \left[1 - \left(1 - \frac{T_1}{T_2} \right) \exp(-cx^2) \right]^{\frac{1}{2}} = 1 - \sum_{n=1}^{\infty} A(n) \left(1 - \frac{T_1}{T_2} \right)^n \exp(-ncx^2)$$

Putting this in the integral

$$F(\omega) = \int_{-\infty}^{\infty} \sqrt{T_2} \left[1 - \sum_{n=1}^{\infty} A(n) \left(1 - \frac{T_1}{T_2} \right)^n \exp(-ncx^2) \right] \exp(-i\omega x) dx$$

Using the cosine transform, because of symmetry, and the aperture limits

$$F(\omega) = 2\sqrt{T_2} \int_0^{x_f} \cos \omega x dx - 2\sqrt{T_2} \sum_{n=1}^{\infty} A(n) \left(1 - \frac{T_1}{T_2} \right)^n \int_0^{\infty} \exp(-ncx^2) \cos \omega x dx$$

Integrating

$$F(\omega) = 2\sqrt{T_2} x_f \text{sinc}(\omega x_f) - \sqrt{T_2} \sum_{n=1}^{\infty} A(n) \left(1 - \frac{T_1}{T_2} \right)^n \frac{\sqrt{\pi}}{\sqrt{nc}} \exp(-\omega^2/4nc)$$

This pulse may also have a light center in the form

$$f_2(x) = T_1 + (T_2 - T_1) \exp(-cx^2)$$

The expansion and analysis using this pulse is very similar to that of $f_1(x)$.

We now obtain the image of $f_1(x)$, after passing it through a symmetric, sharp cutoff occluding filter (see Fig. 3) centered in the frequency plane whose characteristic is

$$\begin{aligned} G(\omega) &= 1 & (\omega_1 \leq \omega \leq \infty) \\ G(\omega) &= 0 & (0 < \omega < \omega_1) \end{aligned}$$

The distribution in the image plane is given by the following transform

$$h_1(z) = \frac{1}{2\pi} \int_{-\infty}^{\infty} F(\omega) G(\omega) \exp(i\omega z) d\omega$$

Again, for reasons of symmetry, we may use the cosine transform

$$\begin{aligned} h_1(z) &= \frac{1}{\pi} \int_{\omega_1}^{\infty} F(\omega) \cos(\omega z) d\omega \\ &= \frac{2\sqrt{T_2}}{\pi} x_f \int_{\omega_1}^{\infty} \text{sinc}(\omega x_f) \cos(\omega z) d\omega \\ &\quad - \frac{\sqrt{T_2} \sqrt{\pi}}{\pi} \int_{\omega_1}^{\infty} \sum_{n=1}^{\infty} A(n) \left(1 - \frac{T_2}{T_1}\right)^n \frac{1}{\sqrt{nc}} [\exp(-\omega^2/4nc)] \cos(\omega z) d\omega \\ &= \frac{2\sqrt{T_2}}{\pi} x_f \int_0^{\infty} \text{sinc}(\omega x_f) \cos(\omega z) d\omega - \frac{2\sqrt{T_2}}{T_2} x_f \int_0^{\omega_1} \text{sinc}(\omega x_f) \cos(\omega z) d\omega \\ &\quad - \frac{\sqrt{T_2}}{\sqrt{\pi}} \sum_{n=1}^{\infty} A(n) \left(1 - \frac{T_1}{T_2}\right)^n \\ &\quad \times \frac{1}{\sqrt{nc}} \left[\int_0^{\infty} \exp(-\omega^2/4nc) \cos(\omega z) d\omega - \int_0^{\omega_1} \exp(-\omega^2/4nc) \cos(\omega z) d\omega \right] \end{aligned}$$

Applying the trigonometric identity

$$\sin(\omega x_f) \cos(\omega z) = 1/2 \sin(x_f + z)\omega + \sin(x_f - z)\omega$$

and integrating, we get

$$\begin{aligned}
 h_1(z) = & \frac{\sqrt{T_2}}{\pi} \left[\frac{\pi}{2} + \frac{\pi}{2} \right] - \frac{\sqrt{T_2}}{\pi} \text{Si} (x_f + z) \omega_1 - \frac{T_2}{\pi} \text{Si} (x_f - z) \omega_1 \\
 & - \frac{\sqrt{T_2}}{\sqrt{\pi}} \sum_{n=1} A(n) \left(1 - \frac{T_1}{T_2} \right) \frac{1}{\sqrt{nc}} \sqrt{n\pi c} \exp (-cnz^2) \\
 & + \frac{\sqrt{T_2}}{\sqrt{\pi}} \sum_{n=1} A(n) \left(1 - \frac{T_1}{T_2} \right)^m \frac{1}{\sqrt{nc}} \int_0^{\omega_1} \exp (-\omega^2/4nc) \cos (\omega z) d\omega
 \end{aligned}$$

Finally, the pulse image is given by

$$\begin{aligned}
 h_1(z) = & \sqrt{T_2} - \frac{\sqrt{T_2}}{\pi} [\text{Si} (x_f + z) \omega_1 + \text{Si} (x_f - z) \omega_1] \\
 & - \sqrt{T_2} \sum_{n=1} A(n) \left(1 - \frac{T_1}{T_2} \right)^n \exp (-cnz^2) \\
 & + \frac{\sqrt{T_2}}{\sqrt{\pi}} \sum_{n=1} A(n) \left(1 - \frac{T_1}{T_2} \right)^n \frac{1}{\sqrt{nc}} \int_0^{\omega_1} \exp (-\omega^2/4nc) \cos (\omega z) d\omega
 \end{aligned}$$

Rewriting the image term in the following form

where $a = \frac{\omega_1}{\sqrt{2c}}$

$$m = z\sqrt{2c}$$

$$\frac{\omega}{\omega_1} = t$$

$$d\omega = \omega_1 dt$$

$$\begin{aligned}
 h_1(a, m) = & \sqrt{T_2} - \frac{\sqrt{T_2}}{\pi} [\text{Si} (x_f\sqrt{2c} + m)a + \text{Si} (x_f\sqrt{2c} - m)a] \\
 & - \sqrt{T_2} \sum_{n=1} A(n) \left(1 - \frac{T_1}{T_2} \right)^n \exp (-nm^2/2) \\
 & + \frac{\sqrt{T_2}}{\sqrt{\pi}} \sum_{n=1} A(n) \left(1 - \frac{T_1}{T_2} \right)^n \frac{a}{\sqrt{2n}} \int_{-1}^1 \exp (-a^2t^2/2n) \cos (amt) dt
 \end{aligned}$$

Since c , the pulse variance is large, then $x_f\sqrt{2c}$ is large and the value of $\text{Si} (x_f\sqrt{2c} \pm m) a$ approaches $\pi/2$. Under this condition, the image reduces to

$$h_1(a, m) = -\sqrt{T_2} \sum_{n=1}^{\infty} A(n) \left(1 - \frac{T_1}{T_2}\right) \exp(-nm^2/2) \\ + \frac{\sqrt{T_2}}{\sqrt{\pi}} \sum_{n=1}^{\infty} A(n) \left(1 - \frac{T_1}{T_2}\right)^n \frac{a}{\sqrt{2n}} \int_{-1}^1 \exp(-a^2 t^2/2n) \cos(amt) dt$$

At this point, it is necessary to compute the values of the integral

$$\frac{a}{\sqrt{2\pi n}} \int_{-1}^1 \exp(-a^2 t^2/2n) \cos(amt) dt$$

Upon receiving these values, it is then possible to normalize the total energy of the filtered cases to the unfiltered case.

The cases computed were those where a had the values of $1/4$, $1/2$, 1 , and 2 , and n varied from 1 to 5 ; m was taken in steps of 0.05 from 0 to 3.0 ; T_1 was taken in steps of 0.01 from 0 to 0.99 ; and T_2 was set at 1.0 .

The normalization procedure is the following

$$\int_{-\infty}^{\infty} \frac{h^2(a, m)}{T_2} = I(a, m)$$

which is normalized to the total energy of the unfiltered pulse $A_p = I(0, m)$ where $a = 0$. Therefore, the normalization factor is

$$N = \frac{A_p}{I(a, m)}$$

The area of the filtered image, $I(a, m)$, is approximated by Simpson's rule for normalization purposes.

Representative results of the computations were plotted (see Fig. 4, a through h).

The parameters relating k , the linear frequency, and c , the pulse variance for a 's varying from 0 to 2 , are plotted in Fig. 5. This relationship is defined by

$$c = \frac{2\pi^2 k^2}{a^2}$$

For the entire range of edge contrast (variation of T_1), the smaller filter sizes give the expected results, i.e., increased normalized contrast for increased filter size. The larger filter sizes give rather unexpected and varying results for changing contrast. A full explanation for this phenomenon cannot be made without further study.

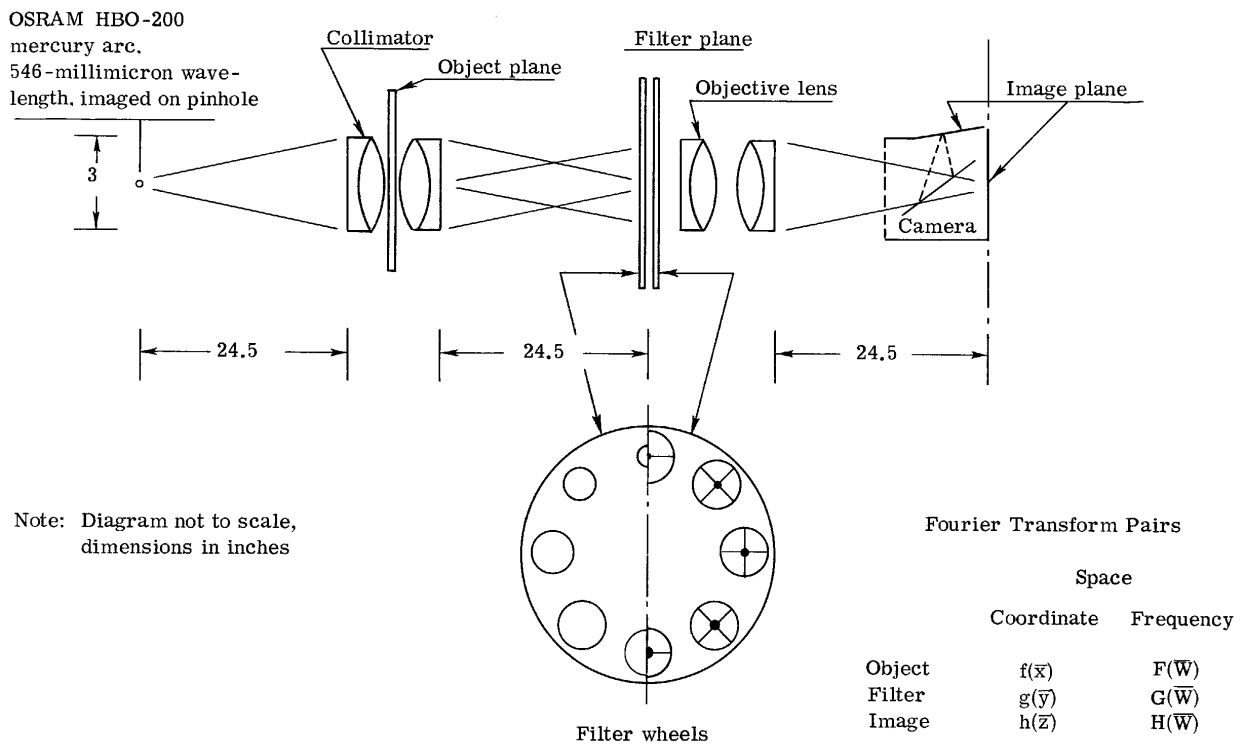
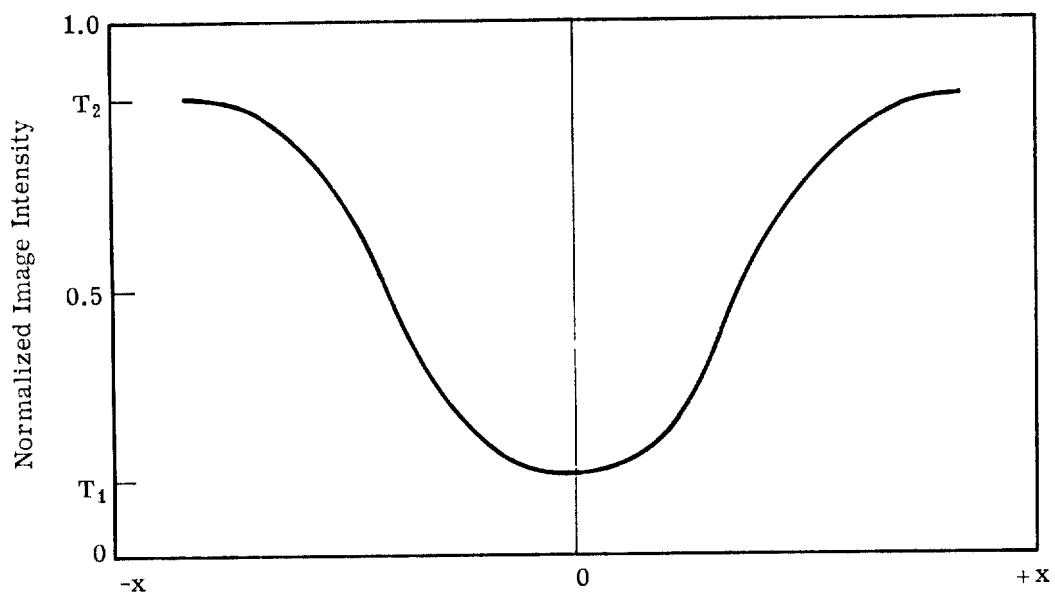
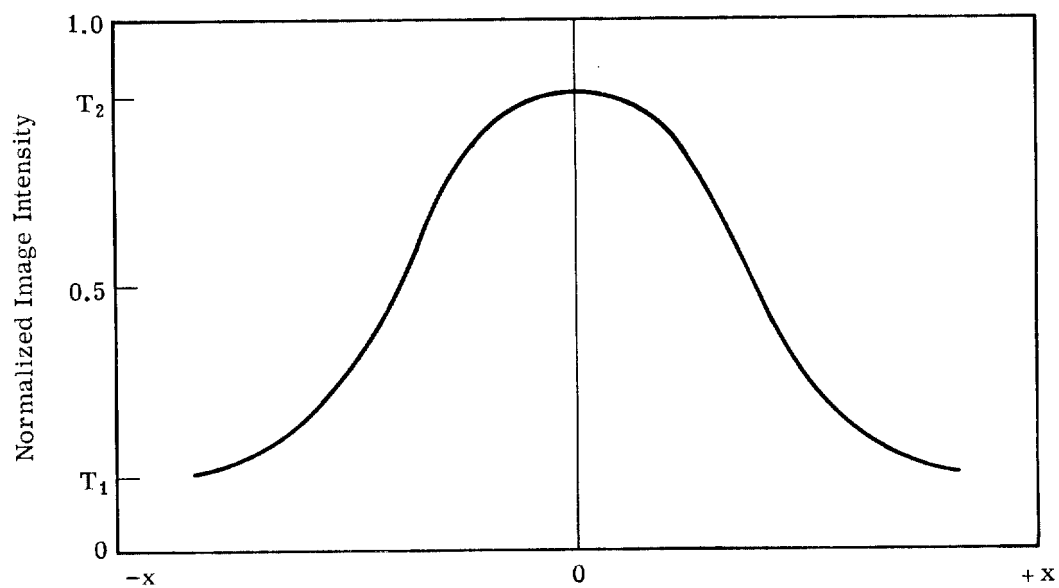


Fig. 1 — Linear, coherent optical system showing focal planes of interest and defining the notation and location of the Fourier transform planes



(a) Dark-centered pulse



(b) Light-centered pulse

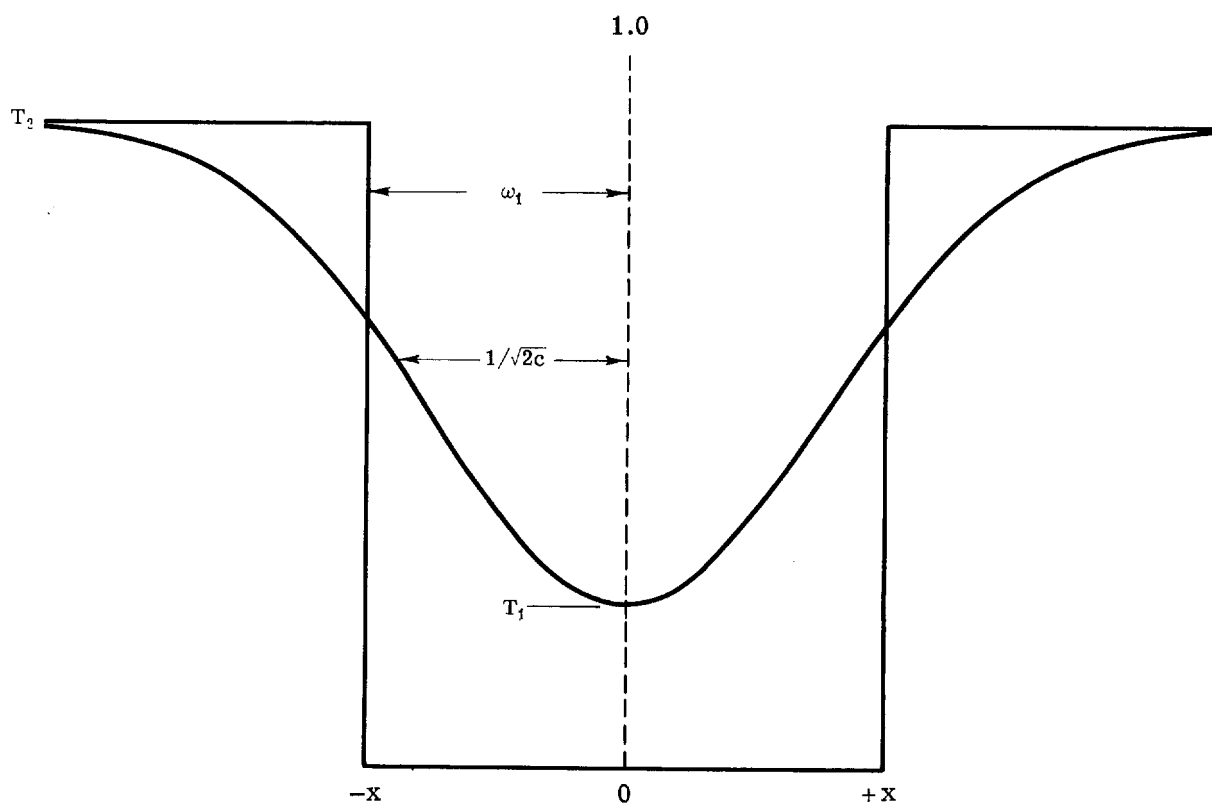
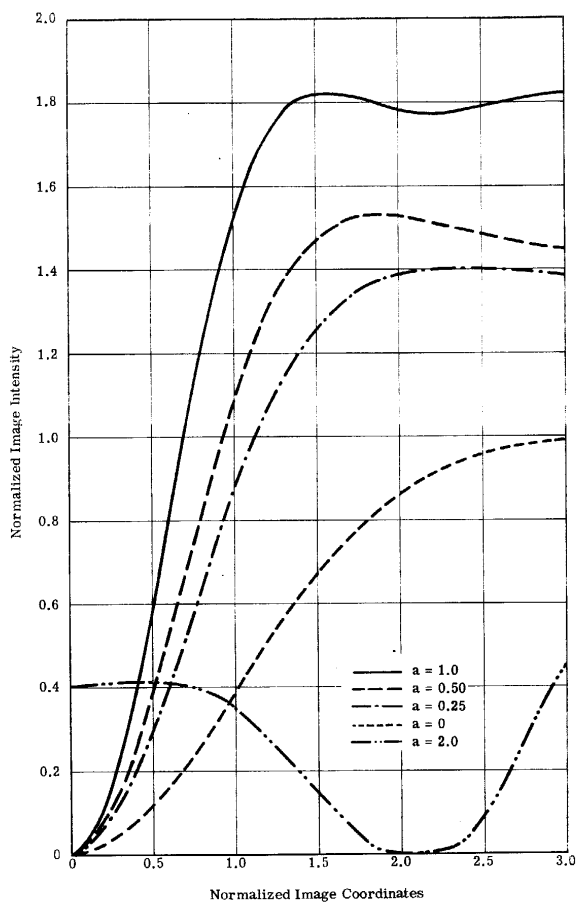
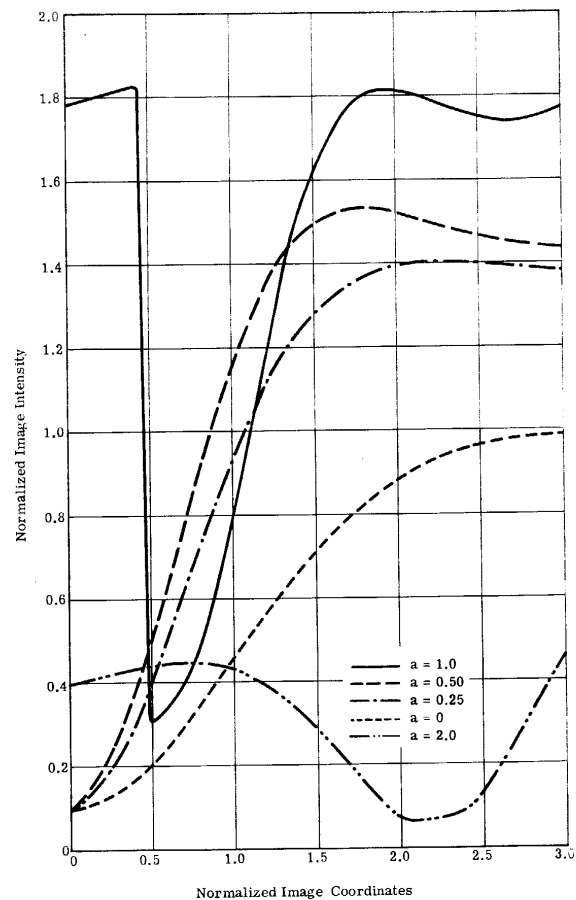


Fig. 3 — Intensity distribution of a dark-centered Gaussian spatial pulse with an occluding spatial filter of radius ω_1 , showing some of the important pulse and filter constants

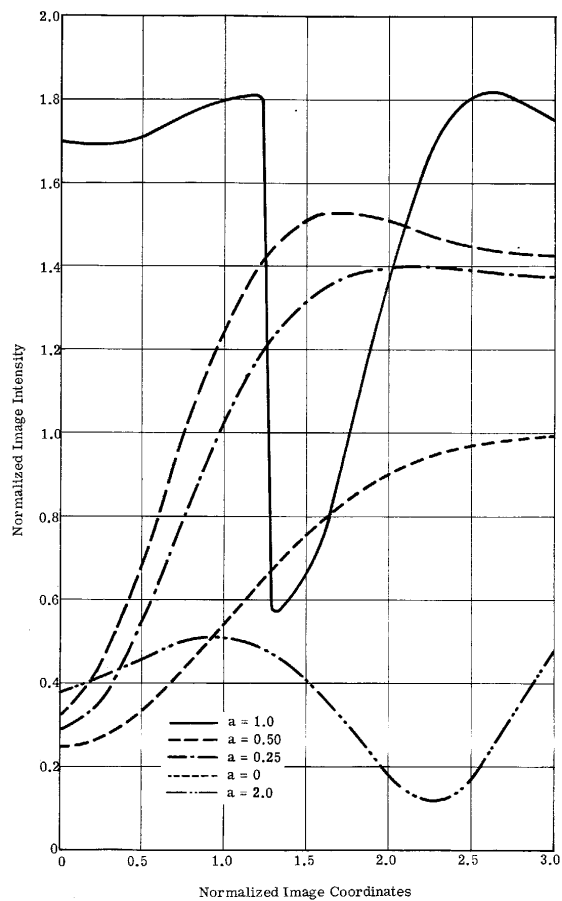


(a) $T_1 = 0$

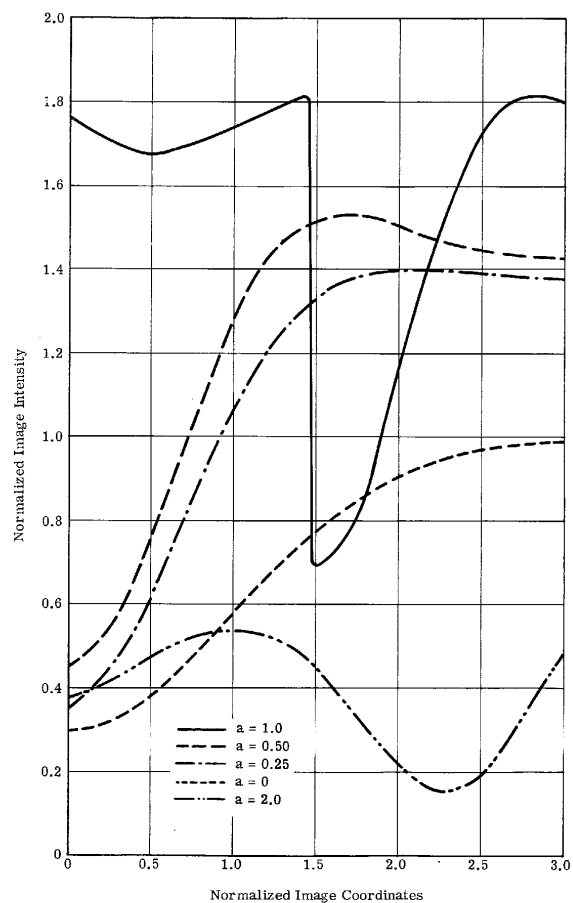


(b) $T_1 = 0.1$

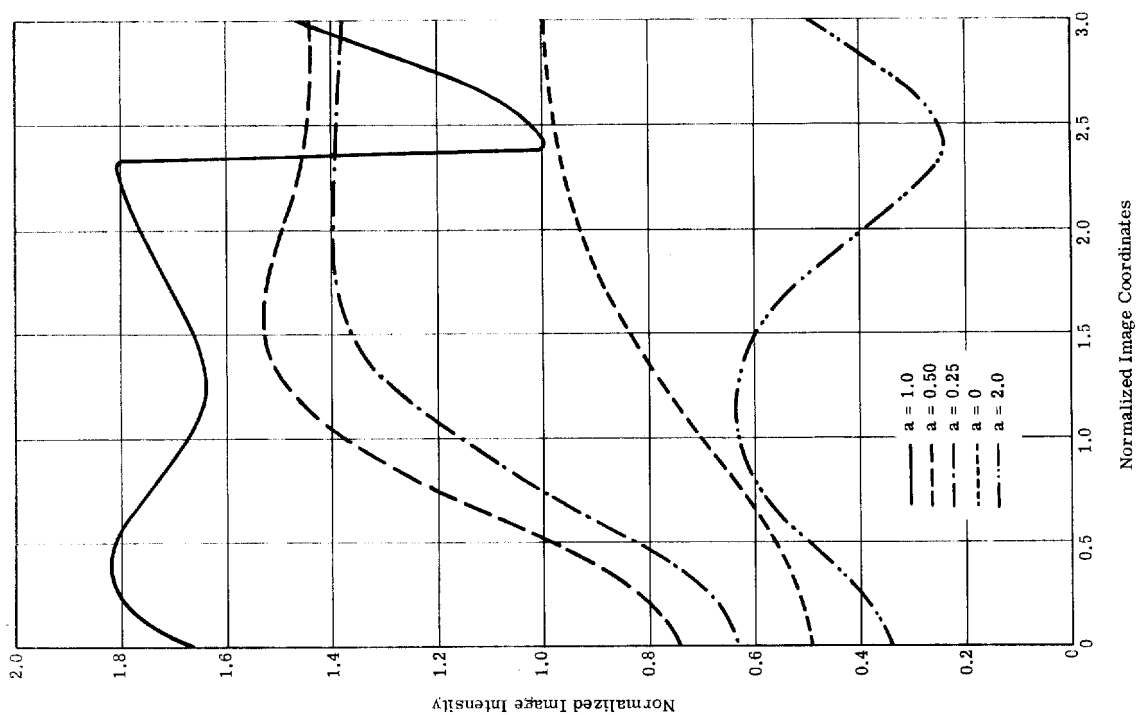
Fig. 4 — Images of nonsharp Gaussian pulses of varying minimum transmissive level, filtered with occluding spatial filters in a linear, coherent optical system



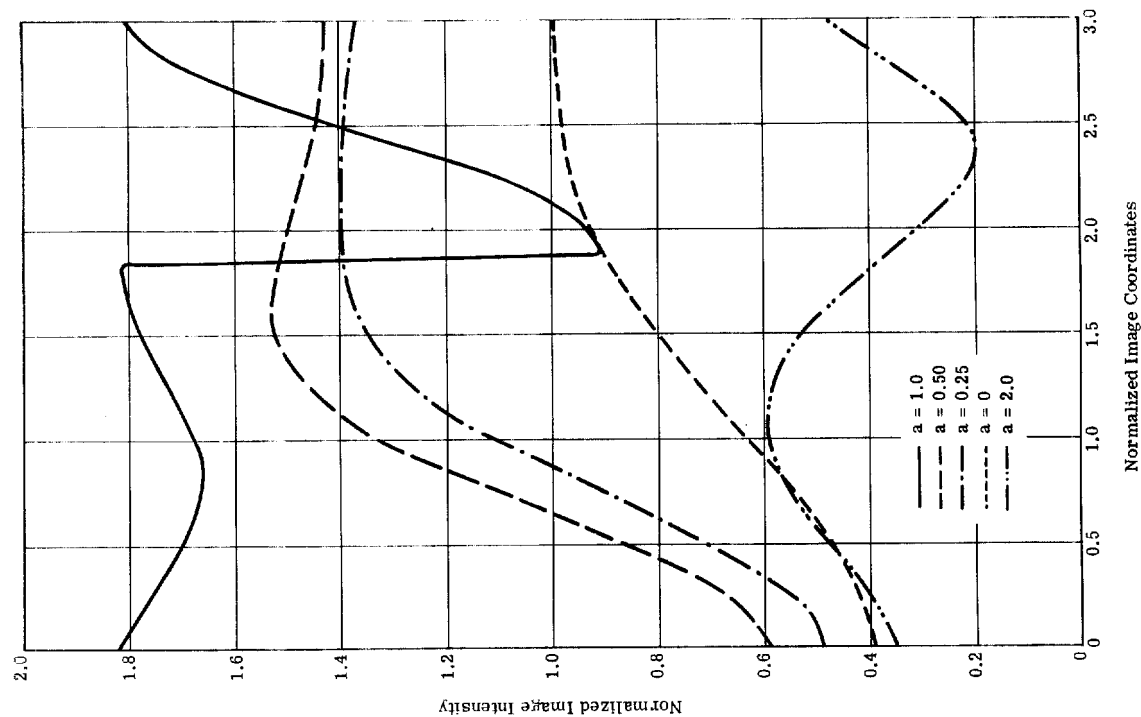
(c) $T_1 = 0.25$



(d) $T_1 = 0.30$

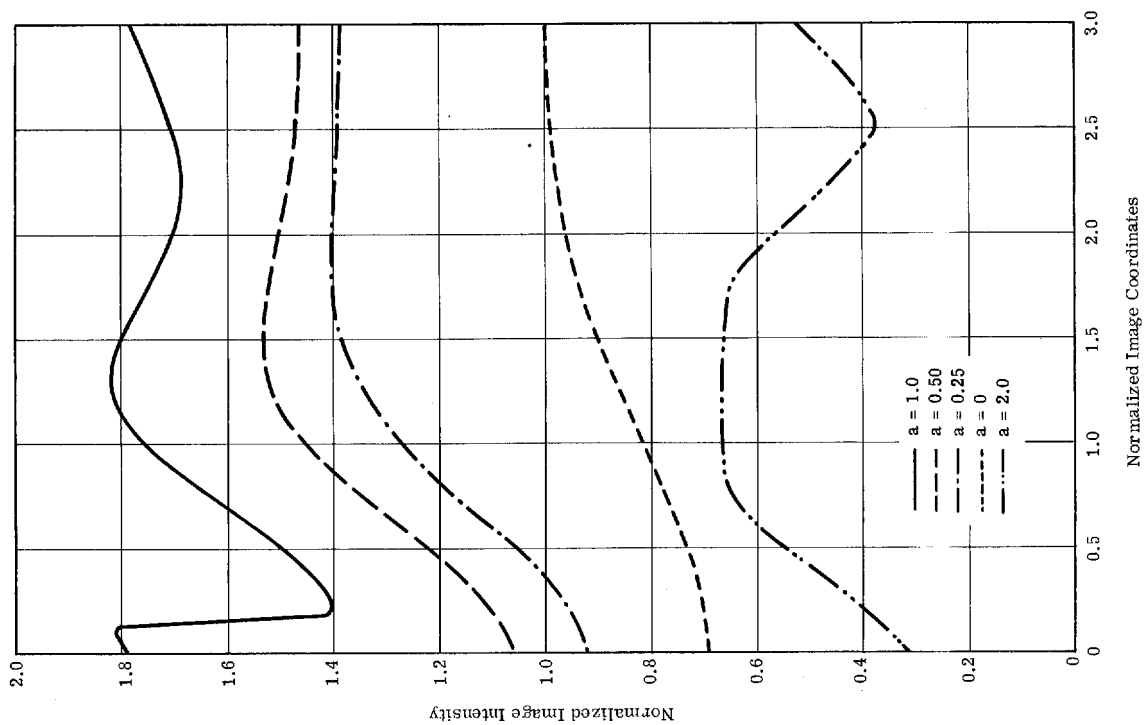


(f) $T_1 = 0.5$

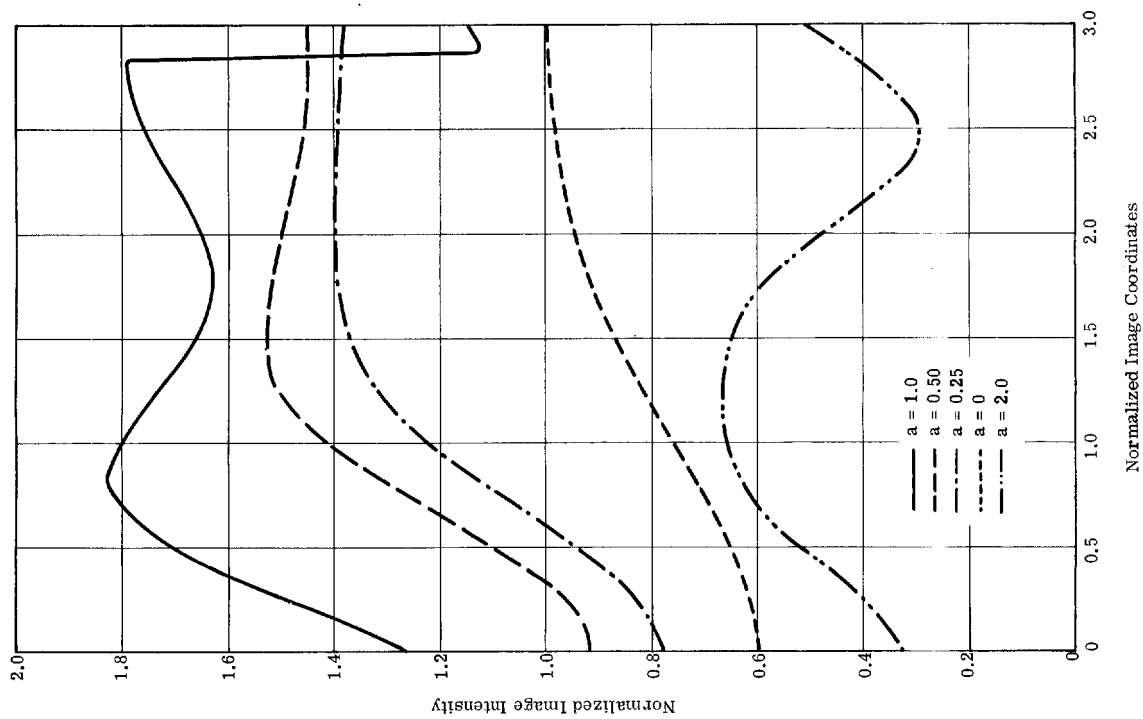


(e) $T_1 = 0.4$

Fig. 4 — (Cont.)



(h) $T_1 = 0.7$



(g) $T_1 = 0.6$

Fig. 4 — (Cont.)

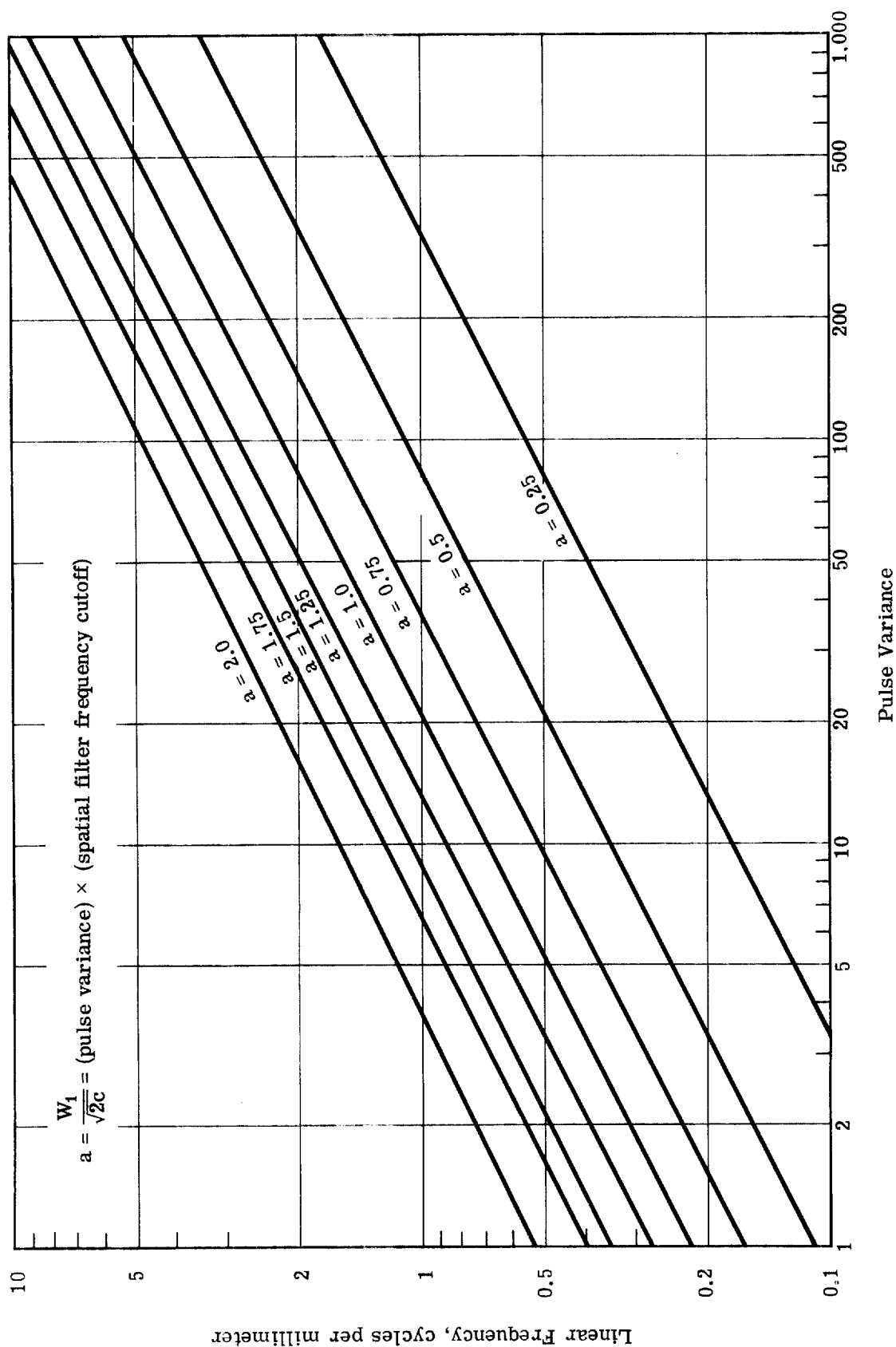


Fig. 5 — Parameters relating the linear frequency, k , the pulse variance, c , for values of $a = 0, 0.25, 0.50, 1.0, 1.5$, and 2.0

3. EXPERIMENTAL FILTERING OF A NONSHARP EDGE

In order to substantiate the theoretical work, an experiment was designed with conditions approximating the analysis.

Instead of a pulse, a filmed nonsharp edge was used as an object. This was placed in the object plane of the image enhancement viewer. Though the shape of this pulse had first been assumed to be Gaussian, subsequent traces revealed a number of un-Gaussian characteristics which could well affect the resulting filtered traces.

Because an edge and not a pulse was used, the filters placed in the object plane did not have to be circular (the frequency distribution being one dimensional). The occluding filters used were pieces of drill rod whose width was accurately known. These filters were then carefully centered in the frequency (or filter) plane.

Using a scanning photometer whose slit width was minimized to the point where, at maximum photometer sensitivity, using the largest filter, 100 percent deflection on the recorder (5-millivolt range) could be reached. The edge was then traced with the photometer placed in the image plane with its slit parallel with the edge. First, the image of the edge with no occluding filter and the images of the edge with filters corresponding to $a = 1.5$ and $a = 2.5$ were traced.

The actual traces for the three cases are shown in Fig. 6. (The two filtered cases are expanded by a factor of 10 in the intensity scale.)

The resulting filtered cases were normalized to the area under the unfiltered curve in the same manner as used in the theoretical traces. The resulting curves are plotted in Fig. 7. Because the normalized cases are meant to be compared with the theoretical Gaussian, only the part of the edge corresponding to a pulse (center $1/\sqrt{2}c$ distance from the inflection point) is taken.

Because of differences between the experimental edge and the Gaussian pulse taken in part 1, and the limitations in filter size (it was not possible to obtain smaller filters), no conclusion can be drawn from the results, though a general agreement may be found.

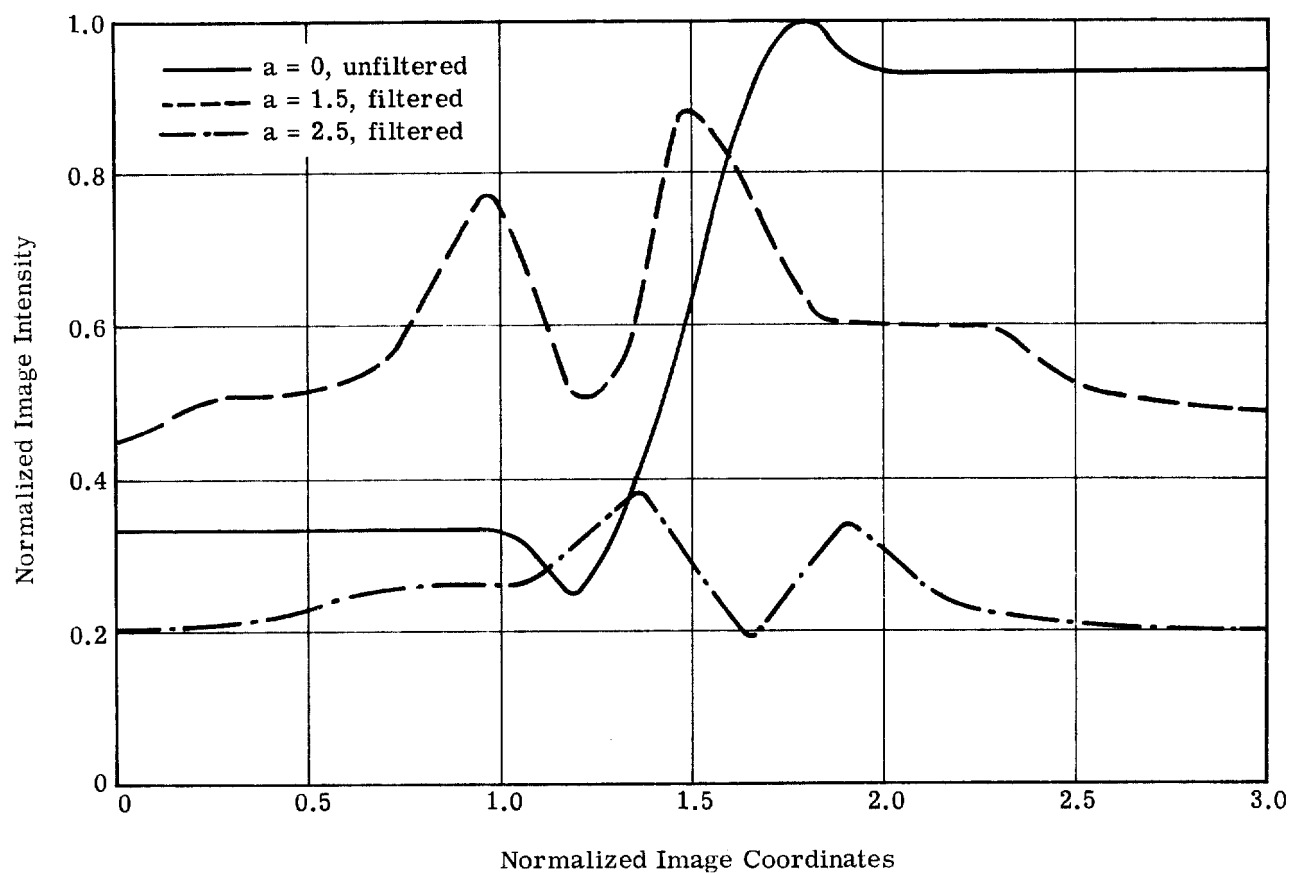


Fig. 6 — Plots of the intensity distribution in the aerial image of an unfiltered and two filtered edges ($a = 1.5$ and 2.5)

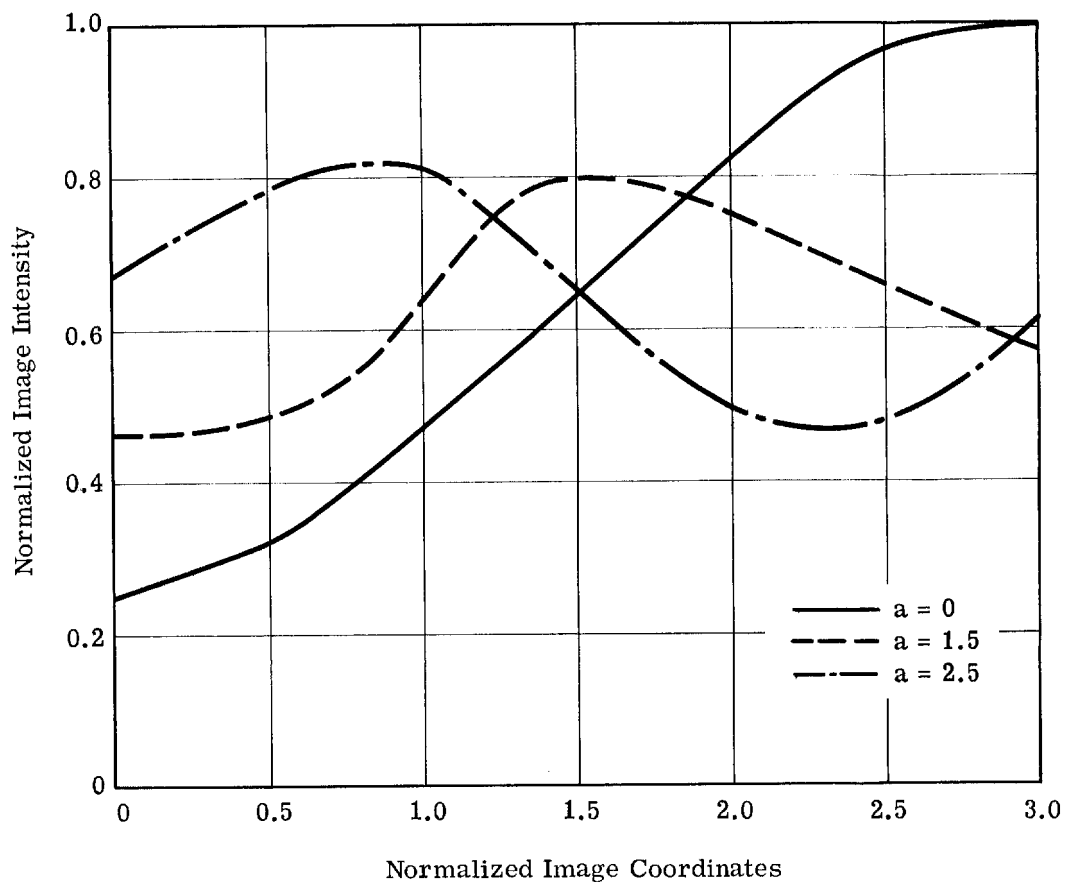


Fig. 7 — Normalized (to total area under unfiltered curve) intensity distribution of the image of two experimentally filtered edges

4. EDGE ENHANCEMENT THROUGH EXPOSURE ADDITION

The next area to be investigated was that of actually applying filtering techniques in order to enhance an edge on a photographic emulsion. This edge may be enhanced in two different ways: (1) increase in contrast, and/or (2) increase in slope.

Two methods for producing such enhancement using the image enhancement viewer have been considered. The first is called exposure addition. In this method, an unfiltered edge is exposed on an emulsion, after which an occluding filter is placed in the system and, without changing the position of either the edge or the film, a second exposure is made on the same frame. The second method is transmission multiplication. Here, two exposures are made on two separate frames; one exposure is unfiltered, the other is filtered to some degree. These two frames are then combined, using some sort of enlarging technique, in various proportions. Obviously, the difficulty in this method is the alignment of the two negatives, which is quite critical. This must be done with an accuracy that entails a great deal of technical ability.

It was possible to do some work in the area of exposure addition, using the test edges from the previous area, but because of time limitation, it was impossible to do any transmission multiplication.

An edge was exposed, using several occluding filters with varying exposure times, mixing the filtered and unfiltered parts. These edges were then microdensitometered on our Intectron instrument. For these traces, an effective 3-micron slit was used. The results of these traces have been recorded in Table 1.

Tables 1 and 2 are based upon exposures 1 to 19. The slopes (Table 1) and edge contrasts (Table 2) are those read, averaged, and weighted from several microdensitometer traces, varied for relative slit position with the edge. Included is the sensitometric curve relevant for the longer exposure times. Given also are the exposure times and the maximum densities (upper point through which the slope passes). As can be seen, some of these values are well up on the shoulder of the sensitometric curve (Fig. 8). All of the exposures were on 70-mm Panatomic-X film. A plot of the measured edge slopes against the ratio of filtered to unfiltered exposure time is plotted in Fig. 9.

From this data it may be concluded that, with correct mixtures of filtered and unfiltered exposures, it is possible to equal or even slightly surpass the slope of the original edge.

Table 1 — Slope of Traced, Enhanced Edges

Exposure No.	Filter Diameter, in.	Average Slope	Unfiltered Time, sec	Filtered Time, sec
1	—	4.5	1/2	—
2	—	3.5	1	—
3	0.015	3.2	1/2	1
4	0.015	2.5	1/2	2
5	0.015	3.6	1/2	4
6	0.015	4.3	1	1
7	0.015	2.8	1	2
8	0.015	2.4	1	4
9	0.025	2.8	1/2	2
10	0.025	4.0	1/2	4
11	0.025	4.1	1/2	8
12	0.025	2.8	1	4
13	0.025	2.9	1	8
14	0.041	2.8	1/2	4
15	0.041	3.1	1/2	8
16	0.041	5.0	1/2	16
17	0.041	3.2	1	4
18	0.041	2.0	1	8
19	0.041	1.9	1	16

Table 2 — Contrast of Traced, Enhanced Edges

Exposure No.	Minimum Density	Maximum Density	Contrast
1	0.60	1.50	0.90
2	0.95	1.20	0.85
3	0.85	1.45	0.60
4	1.35	1.80	0.45
5	1.55	1.90	0.35
6	1.15	1.85	0.70
7	1.50	2.00	0.50
8	1.40	1.90	0.50
9	0.80	1.55	0.75
10	1.20	1.70	0.50
11	1.00	1.60	0.60
12	1.10	1.80	0.70
13	1.35	1.85	0.50
14	0.85	1.55	0.70
15	0.75	1.50	0.75
16	0.90	1.55	0.65
17	0.95	1.70	0.75
18	1.30	1.80	0.50
19	1.65	2.25	0.60

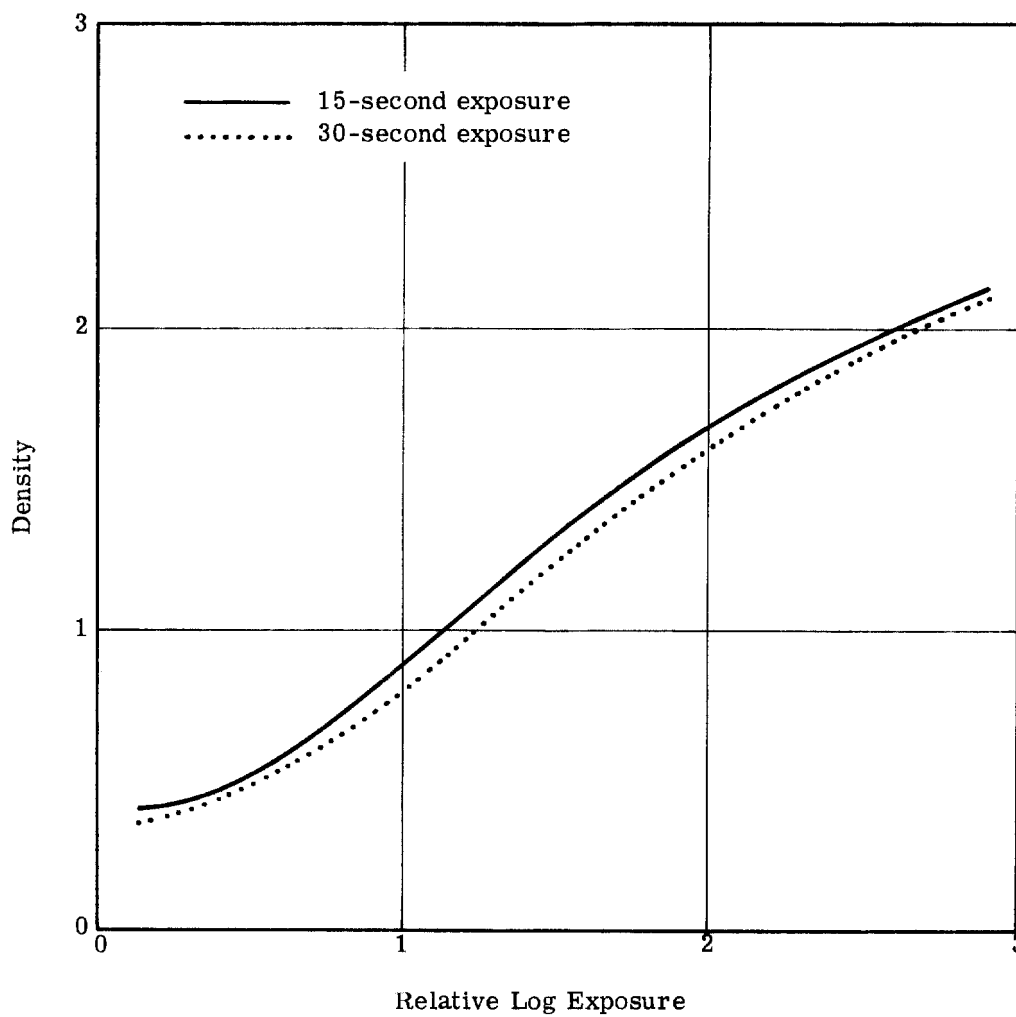


Fig. 8 — Sensitometric curves for enhanced edges on Panatomic-X film developed in D-19 for 6 minutes

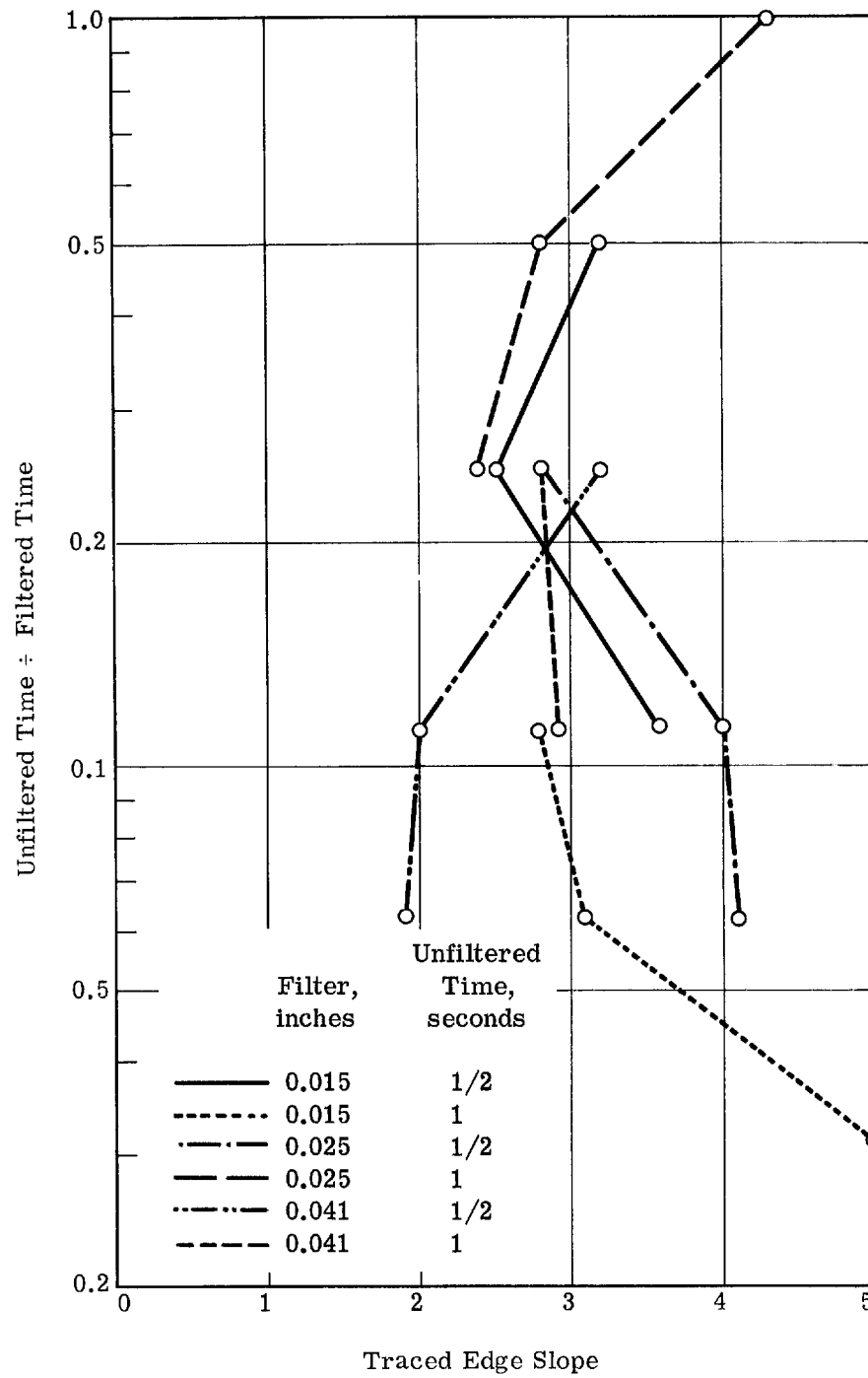


Fig. 9 — Change of slope of an edge with a varying ratio of unfiltered time to filtered time using the technique of exposure addition

5. APPLICATION OF SPATIAL FILTERING TO THE EXAMINATION OF AERIAL PHOTOGRAPHS

As part of the studies with the image enhancement viewer, it was considered desirable to examine some aerial negatives with various degrees of spatial filtering. The reason for this was that it is sometimes thought that details below the limit of detection can be brought above this threshold by suitable filtering. Also, it is conceivable that recognition of poorly defined objects might be improved by a controlled filtering which causes ringing at the edges.

When the detail to be detected has a well defined spectrum, or a known pattern, spatial filtering has definite advantages. For example, a sinusoidal frequency of low modulation, recorded photographically, may be invisible against a grainy background, but by use of a spatial filter permitting only that frequency to pass, the grain noise is eliminated from the reconstituted image and the sinusoidal pattern may be seen. To be more precise, only those components of the grain frequency spectrum which lie in the passband of the filter remain to obscure the wanted image, and if the grain spectrum is flat, this gives a great improvement in signal-to-noise ratio. However, this is an ideal case for the use of filtering, since the signal spectrum is concentrated at one point in the diffraction plane, while the noise spectrum is widely distributed across the plane. When the object is more complex—for example, a square wave instead of a sine wave—its spectrum theoretically extends to infinity, and noise cannot be reduced without distorting the signal to some degree. If the significant feature of the object, however, is its repetitive nature and not the shape of the waves, the filtering can be as effective as for the sinusoidal pattern. For aerial scenes in general, little or no improvement can be expected from spatial filtering, because the details, consisting of sharp edged lines or similar, simple, nonrepetitive shapes, have very complex spectra. Filtering to reduce noise can only be effective if the objects of interest have simple, known spectra, for which individual filters can be made in advance.

To test these ideas under a realistic approximation to operational conditions, the following experiment was carried out with a setup which was being used in another program. Simulated aerial photographs were made by photographing a transparency made under controlled tone reproduction conditions from a large scale aerial negative. The original negative scale was 1:2,000 and the reduction factor, using a 6-inch lens, was 20 to 1. Thus the copy negatives were at 1:40,000 scale. Uniform fogging light from a beam splitter was introduced during the copying, to reduce the luminance scale of the transparency to approximately 5 to 1, simulating an aerial scene viewed from a high altitude. Negatives were made on SO-243 emulsion, varying the lens-film transfer function by changing the lens aperture. These lens-film transfer functions are shown in Fig. 10; for these values of spatial frequency cutoff, granularity is not obtrusive when looking for detail in the negatives. Thus a series of negatives were available in which the quality of definition showed a progressive deterioration of known amount. The intention was to apply various kinds of filtering, and if any improvement could be seen, to equate this to the quality of the next best negative. Thus any effect of the filtering could be approximately evaluated in terms of the definition of conventionally viewed photographs.

The original 1:40,000 scale negatives, being only 1 centimeter in diameter, were enlarged 6 \times , the resulting positive transparencies being more convenient for viewing in the spatial filtering apparatus. (It was known, from work in the other programs referred to above, that the enlarging process introduced no significant loss of quality even for the best negative.)

After repeated trials of filtering, both high pass and low pass, it was concluded that no choice of frequency band enabled anything to be seen which could not be seen as well or better in normal viewing by incoherent light. Indeed, due to the disturbing effect of the ringing around small particles of dirt which had not been completely removed from the negatives or filtered from the fluid, the incoherent viewing was always preferred. In a few instances it was felt that the edges of isolated objects such as trucks might have been more clearly defined when using a high pass filter, but this effect was so small (if it existed) that a followup with more precise experimentation was not justified.

This negative conclusion is in accordance with the theoretical expectations, as discussed earlier in this section.

It should perhaps be stressed that these findings do not imply that coherent light techniques have no value for the detection of previously known patterns.

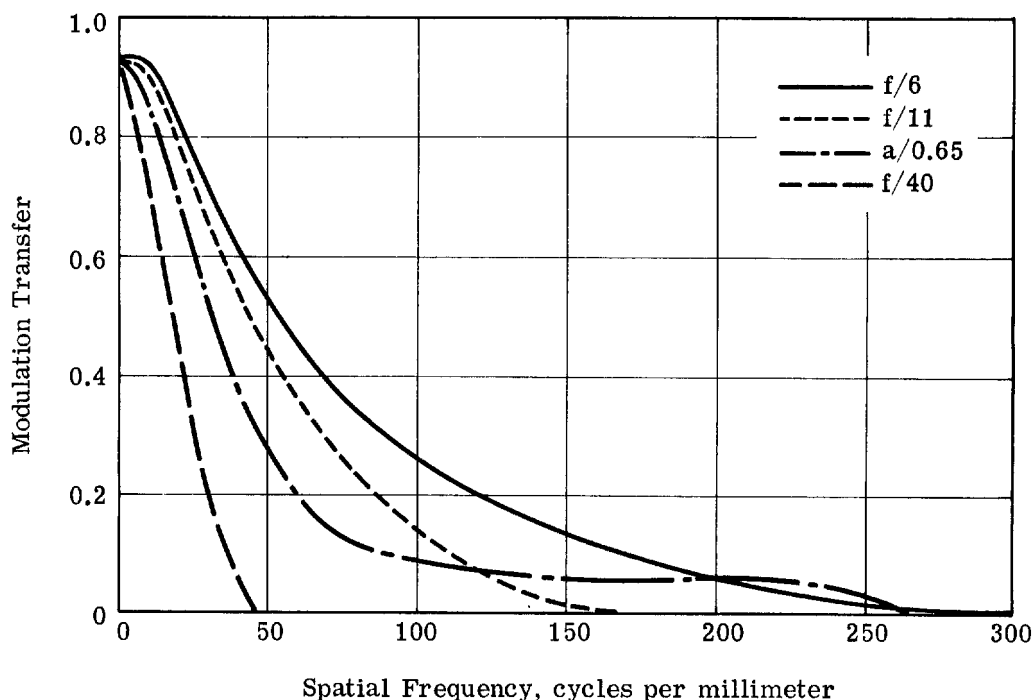


Fig. 10 — Four lens-film transfer functions using SO-243 film

25X1B

Next 1 Page(s) In Document Exempt

SPECIAL HANDLING

ENCL TO.

OSA - 5188-64

SHC64-9043-671

Copy No. 1

9 November 1964

BB 425
T.O. #4
[Signature]

Dear John:

Transmitted herewith are five (5) copies of the DD-250 form covering the transmittal of the Final Report - A Study of Spatial Filtering Using the Image Enhancement Viewer - under Contract BB-425, Task Order No. 4.

Five (5) copies of the report are also enclosed.

25X1A Would you please execute (2) copies of the DD-250 form and return them to [Redacted]

Very truly yours,

25X1A

[Redacted Signature Box]

Contracts Manager

pv
Encls: 10

SPECIAL HANDLING

SECRET
(When Filled In)

Approved For Release 2002/09/04 : CIA-RDP67B00820R000300110031-7
CONTRACT INSPECTION REPORT

TO:

ENGINEERING SECTION/CB/PD/OL

BB425

DATE

1 Nov 64

INSPECTION REPORT NO. (If final, so state)

12

ESTIMATED COMPLETION DATE

30 Nov 64

NAME OF CONTRACTOR

Itek Corporation

TYPE OF COMMODITY OR SERVICE

Optical Image Enhancement Device

THE CONTRACTOR IS ON SCHEDULE

☐

YES

☒

NO

PER CENT OF WORK COMPLETED

98%

THE CONTRACTOR WILL PROBABLY REMAIN WITHIN ALLOCATED FUNDS ☒ YES ☐ NO IF ANSWER IS "NO" ADVISE RECOMMENDATION AND/OR ACTION OF SPONSORING OFFICE, ON REVERSE HEREOF. IF KNOWN, INDICATE MAGNITUDE OF ADDITIONAL FUNDS INVOLVED.

HAS AN INTERIM REPORT, FINAL REPORT, PROTOTYPE, OR OTHER END ITEM BEEN RECEIVED FROM THE CONTRACTOR DURING THE PERIOD? ☒ YES ☐ NO (If yes, give details on reverse side.)

An unsatisfactory final report has been submitted. Revisions to make it acceptable are now being prepared. Expected delivery is Nov. 1964.

HAS GOVERNMENT-OWNED PROPERTY BEEN DELIVERED TO CONTRACTOR DURING THIS PERIOD? ☐ YES ☒ NO (If yes, indicate items, quantity, and cost on reverse side.)

OVERALL PERFORMANCE OF CONTRACTOR

1. ☐ OUTSTANDING

3. ☐ ABOVE AVERAGE

5. ☒ BELOW AVERAGE 7. ☐ UNSATISFACTORY

2. ☐ EXCELLENT

4. ☐ AVERAGE

6. ☐ BARELY ADEQUATE

IF OVERALL PERFORMANCE OF CONTRACTOR IS UNSATISFACTORY OR BARELY ADEQUATE, INDICATE REASONS ON REVERSE SIDE.

RECOMMENDED ACTION

☒ CONTINUE AS PROGRAMMED

☐ WITHHOLD PAYMENT PENDING SATISFACTORY PERFORMANCE

☐ TERMINATE

☐ OTHER (Specify)

IF TERMINATION IS RECOMMENDED OR IF THIS IS A FINAL REPORT ATTACH COMMENTS IN NARRATIVE FORM ON CONTRACTOR'S PERFORMANCE AND CERTIFY THAT ALL DELIVERABLE ITEMS UNDER THE CONTRACT HAVE BEEN RECEIVED. THESE INCLUDE, WHERE APPLICABLE, THE FOLLOWING:

ITEM	REC'D	DOES NOT APPLY	ITEM	REC'D	DOES NOT APPLY
PROTOTYPES			MANUALS		
DRAWINGS AND SPECIFICATIONS			FINAL REPORT		
PRODUCTION AND/OR OTHER END ITEMS			SPECIAL TOOLING		
			OTHER GOVERNMENT PROPERTY		

DATE OF LAST CONTACT WITH CONTRACTOR

10 Oct 64

S

DIVISION

P&DS

INSPECTOR'S EXTENSION

3308

S

SECRET
(When Filled In)

Approved For Release 2002/09/04 : CIA-RDP67B00820R000300110031-7 CONTRACT INSPECTION REPORT		CONTRACT NO. BB 425	TASK NO. 4		
TO: ENGINEERING SECTION/CB/PD/OL <div style="text-align: center; font-size: 1.2em;">11/23/64</div>		DATE 1 Oct 64 INSPECTION REPORT NO. (If final, so state) 11 ESTIMATED COMPLETION DATE Oct 1964			
NAME OF CONTRACTOR Itek Corp.					
TYPE OF COMMODITY OR SERVICE Optical Image Enhancement Device					
THE CONTRACTOR IS ON SCHEDULE <input type="checkbox"/> YES <input checked="" type="checkbox"/> NO		THE CONTRACTOR WILL PROBABLY REMAIN WITHIN ALLOCATED FUNDS <input checked="" type="checkbox"/> YES <input type="checkbox"/> NO IF ANSWER IS "NO" ADVISE RECOMMENDATION AND/OR ACTION OF SPONSORING OFFICE, ON REVERSE HEREOF. IF KNOWN, INDICATE MAGNITUDE OF ADDITIONAL FUNDS INVOLVED.			
PER CENT OF WORK COMPLETED <u>98%</u>					
HAS AN INTERIM REPORT, FINAL REPORT, PROTOTYPE, OR OTHER END ITEM BEEN RECEIVED FROM THE CONTRACTOR DURING THE PERIOD? <input checked="" type="checkbox"/> YES <input type="checkbox"/> NO (If yes, give details on reverse side.)					
HAS GOVERNMENT-OWNED PROPERTY BEEN DELIVERED TO CONTRACTOR DURING THIS PERIOD? <input type="checkbox"/> YES <input checked="" type="checkbox"/> NO (If yes, indicate items, quantity, and cost on reverse side.)					
OVERALL PERFORMANCE OF CONTRACTOR					
1. <input type="checkbox"/> OUTSTANDING 3. <input type="checkbox"/> ABOVE AVERAGE 5. <input checked="" type="checkbox"/> BELOW AVERAGE 7. <input type="checkbox"/> UNSATISFACTORY 2. <input type="checkbox"/> EXCELLENT 4. <input type="checkbox"/> AVERAGE 6. <input type="checkbox"/> BARELY ADEQUATE					
IF OVERALL PERFORMANCE OF CONTRACTOR IS UNSATISFACTORY OR BARELY ADEQUATE, INDICATE REASONS ON REVERSE SIDE.					
RECOMMENDED ACTION					
<input checked="" type="checkbox"/> CONTINUE AS PROGRAMMED <input type="checkbox"/> WITHHOLD PAYMENT PENDING SATISFACTORY PERFORMANCE <input type="checkbox"/> TERMINATE <input type="checkbox"/> OTHER (Specify)					
IF TERMINATION IS RECOMMENDED OR IF THIS IS A FINAL REPORT ATTACH COMMENTS IN NARRATIVE FORM ON CONTRACTOR'S PERFORMANCE AND CERTIFY THAT ALL DELIVERABLE ITEMS UNDER THE CONTRACT HAVE BEEN RECEIVED. THESE INCLUDE, WHERE APPLICABLE, THE FOLLOWING:					
ITEM	REC'D	DOES NOT APPLY	ITEM	REC'D	DOES NOT APPLY
PROTOTYPES			MANUALS		
DRAWINGS AND SPECIFICATIONS			FINAL REPORT		
PRODUCTION AND/OR OTHER END ITEMS			SPECIAL TOOLING		
			OTHER GOVERNMENT PROPERTY		
DATE OF LAST CONTACT WITH CONTRACTOR <u>0514</u>					
SIO 			DIVISION P&DS		
INSPECTOR'S EXTENSION 3308			S 		

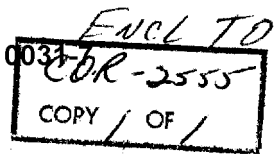
Approved For Release 2002/09/04 : CIA-RDP67B00820R000300110031-7

25X1A

25X1A

The final report on this project was received on 6 Oct 1964. Graphs are not complete and a revision of the report is being requested. Upon receipt of the revised report and verification of data in the report, a final contract inspection report will be completed. If the time required in the past to produce this report can be used to serve as a criterion, two to three interim reports will be forwarded before the final inspection report is forthcoming.

SPECIAL HANDLING



SHC64-9043-524

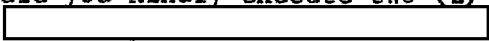
Copy No. 1

ILLEGIB

14 September 1964



Dear Jim:

Transmitted herewith are five (5) copies of the Final Report required under Contract No. BB-425, Task Order No. 4. Enclosed also are five (5) copies of the DD-250 form covering same. Would you kindly execute two (2) copies of the DD-250 form and return them to 



Should you require additional copies, please contact the undersigned.

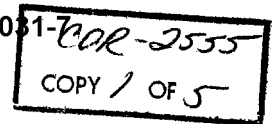
Very truly yours,



Contracts Manager

pv
Attachments 10

SPECIAL HANDLING

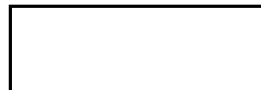


BB 425
T.O. 24
TAP

Project 9043

Final Report

25X1A



Itek Corporation
Lexington, Massachusetts

Table of Contents

	<u>Page</u>
List of Illustrations	2
Table of Symbols	3
A Study of Spatial Filtering Using the Image Enhancement Viewer	4
Theoretical Study of the Effect of Occluding Filters on an Unsharp (Gaussian) Pulse	6
Experimental Filtering of a Non-Sharp Edge	13
Edge Enhancement Through Exposure Addition	15
Application of Spatial Filtering to the Examination of Aerial Photographs	17
Application of Spatial Filtering to Mensuration	20
Table #1	23
Table #2	24
Table #3	25
Figure #1	26
Figure #2	27
Figure #3	28
Figure #4 (a thru h)	29 - 36
Figure #5	37
Figure #6	38
Figure #7	39
Figure #8	40
Figure #9	41

List of Illustrations

- Figure 1: Linear, coherent optical system showing focal planes of interest and defining the notation and location of the Fourier Transform planes.
- Figure 2: Intensity distribution of a dark (top) and a light (bottom) centered Gaussian Spatial Pulse.
- Figure 3: Intensity distribution of a dark centered Gaussian Spatial Pulse with an occluding spatial filter of Radius ω_1 , showing some of the important pulse and filter constants.
- Figure 4: Images of a non-sharp Gaussian pulses of varying minimum transmissive level, filtered with occluding spatial filters in a linear, coherent optical system.
- Figure 5: Parameters relating "k", the linear frequency, "c" the pulse variance for "a" at values of 0, .25, .50, 1.0, 1.5 and 2.0
- Figure 6: Plots of the intensity distribution in the aerial image of an unfiltered and two filtered edges ($a = 1.0$ and 2.5)
- Figure 7: Normalized (to total area under unfiltered curve) intensity distribution of the image of 2 experimentally filtered edges.
- Figure 8: Change of slope of an edge with a varying ratio of unfiltered time to filtered time using the technique of exposure addition.

Table of Symbols

$F(x)$	Intensity Distribution in Object Space
x	Object Coordinate
$F(\omega)$	Amplitude distribution in frequency space
k	Linear frequency
ω	Radian frequency ($2\pi k$) coordinate
$G(\omega)$	Filter characteristic in frequency space
ω_1	Filter cutoff frequency
$H(z)$	Amplitude distribution in image space
z	Image coordinate
T_2	Maximum Transmission level
T_1	Minimum transmission level
c	Variance of the Gaussian pulse

A STUDY OF SPATIAL FILTERING USING
THE IMAGE ENHANCEMENT VIEWER

Introduction

25X1A The work under the present phase of the contract consisted of two main parts. The first was the modification of the Image Enhancement Viewer and the testing and calibration of this instrument. The second was the continuance of research, in certain areas, which had been carried out by , while working under previous contracts for the Viewer.

A description of the modified Viewer, along with the methods of testing and calibration is contained in the Operating Manual. Suffice it to say here that the Viewer was put in working order to the specifications listed in the manual.

The following areas of research were investigated:

A non-sharp, Gaussian pluse was theoretically passed through an optical coherent system; its low frequencies were filtered with a high-pass occluding filter, and the final images were plotted.

A filmed non-sharp edge was experimentally filtered using the Viewer, and its image was traced with a scanning photometer. The results were curve fitted, normalized and plotted.

Techniques (in this study, mainly exposure addition) for increasing edge contrast and sharpness using the Viewer were experimentally examined.

The application of various filtering techniques using actual aerial photographs was studied.

Finally, the use of occluding spatial filtering as a tool in the area of photographic mensuration was investigated.

From the study of these five areas, a comprehensive view of the capabilities and limitations of the Image Enhancement Viewer and occluding spatial filtering may be obtained.

Theoretical Study of the Effect of Occluding Filters on an
Unsharp (Gaussian) Pulse

A full description of the Image Enhancement Viewer (Fig. 1) and its basic properties may be found in both the Operation Manual and the Itek Technical Report OD-61-6. In operation it employs coherent illumination permitting a treatment that is linear in amplitude.

Since all object films used in the system are immersed in an index-matching fluid (See Manual) there should be no shift in phase, and the object maybe considered solely in terms of amplitude.

In order to obtain a general idea of the effect of occluding filtering on amplitude objects, a generalized case (considered Gaussian for mathematical simplicity) was considered theoretically. This pulse is transformed into the frequency plane and there filtered by a circular, centered occluding filter of generalized dimension. The resulting distribution is then again transformed into a filtered image, which has been computed and plotted for the range at representative values.

Considering a non-sharp pulse of Gaussian form (Fig. 2)

$$f_1(x) = T_2 - (T_2 - T_1) e^{-cx^2}$$

where $f_1(x)$ is the intensity distribution of a dark centered pulse in the object plane. Its amplitude spectrum in the frequency plane is given by

$$F(\omega) = \int_{-\infty}^{\infty} [f_1(x)]^{1/2} e^{-i\omega x} dx$$

$[f_1(x)]^{1/2}$ may then be rewritten in the following form

$$\left[f_1(x) \right]^{1/2} = \left[T_2 - \left(T_2 - T_1 \right) e^{-cx^2} \right]^{1/2} = \sqrt{T_2} \left[1 - \left(1 - \frac{T_1}{T_2} \right) e^{-cx^2} \right]^{1/2}$$

Expanding, we get

$$\begin{aligned} \left[1 - \left(1 - \frac{T_1}{T_2} \right) e^{-cx^2} \right]^{1/2} &= 1 - \frac{1}{2} \left(1 - \frac{T_1}{T_2} \right) e^{-cx^2} - \frac{1}{2 \cdot 4} \left(1 - \frac{T_1}{T_2} \right)^2 e^{-2cx^2} \\ &\quad - \frac{1 \cdot 3}{2 \cdot 4 \cdot 6} \left(1 - \frac{T_1}{T_2} \right)^3 e^{-3cx^2} - \frac{1 \cdot 3 \cdot 5}{2 \cdot 4 \cdot 6 \cdot 8} \left(1 - \frac{T_1}{T_2} \right)^4 e^{-4cx^2} \\ &\quad - \frac{1 \cdot 3 \cdot 5 \cdot 7}{2 \cdot 4 \cdot 6 \cdot 8 \cdot 10} \left(1 - \frac{T_1}{T_2} \right)^5 e^{-5cx^2} - \dots \end{aligned}$$

Letting the binomial coefficients be

$$A(1) = \frac{1}{2}$$

$$A(4) = \frac{1 \cdot 3 \cdot 5}{2 \cdot 4 \cdot 6 \cdot 8}$$

$$A(2) = \frac{1}{2 \cdot 4}$$

$$A(5) = \frac{1 \cdot 3 \cdot 5 \cdot 7}{2 \cdot 4 \cdot 6 \cdot 8 \cdot 10}$$

$$A(3) = \frac{1 \cdot 3}{2 \cdot 4 \cdot 6}$$

$$\text{Then } \left[1 - \left(1 - \frac{T_1}{T_2} \right) e^{-cx^2} \right]^{1/2} = 1 - \sum_{n=1}^{\infty} A(n) \left(1 - \frac{T_1}{T_2} \right)^n e^{-ncx^2}$$

Putting this in the integral

$$F(\omega) = \int_{-\infty}^{\infty} \sqrt{T_2} \left[1 - \sum_{n=1}^{\infty} A(n) \left(1 - \frac{T_1}{T_2} \right)^n e^{-ncx^2} \right] e^{-i\omega x} dx$$

Using the cosine transform, because of symmetry, and the aperture limits

$$F(\omega) = 2 T_2 \int_0^{x_f} \cos \omega x \, dx - 2 T_2 \sum_{n=1}^{\infty} A(n) \left(1 - \frac{T_2}{T_1}\right)^n \int_0^{\infty} e^{-ncx^2} \cos \omega x \, dx$$

Integrating

$$F(\omega) = 2\sqrt{T_2} x_f \operatorname{sinc}\left(\omega x_f\right) - \sqrt{T_2} \sum_{n=1}^{\infty} A(n) \left(1 - \frac{T_2}{T_1}\right)^n \frac{\sqrt{\pi}}{\sqrt{nc}} e^{-\frac{\omega^2}{4nc}}$$

This pulse may also have a light center in the form

$$f_2(x) = T_1 + \left(T_2 - T_1\right) e^{-cx^2}$$

The expansion and analysis using this pulse is very similar to that of $f_1(x)$.

We then obtain the image of $f_1(x)$, after passing it through a symmetric sharp cutoff occluding filter (Fig. 3)(centered in the frequency plane) whose characteristic is

$$\begin{aligned} G(\omega) &= 1 & \omega_1 \leq \omega \leq \infty \\ &= 0 & 0 < \omega < \omega_1 \end{aligned}$$

The distribution in the image plane is given by the following transform

$$h_1(z) = \frac{1}{2\pi} \int_{-\infty}^{\infty} F(\omega) G(\omega) e^{i\omega x} \, d\omega$$

Again, for reasons of symmetry, we may use the cosine transform

$$\begin{aligned}
 h_1(z) &= \frac{1}{\pi} \int_{\omega_1}^{\infty} F(\omega) \cos(\omega z) d\omega \\
 &= \frac{2\sqrt{T_2}}{\pi} x_f \int_{\omega_1}^{\infty} \text{sinc}(\omega x_f) \cos(\omega z) d\omega \\
 &\quad - \frac{\sqrt{T_2}\sqrt{\pi}}{\pi} \int_{\omega_1}^{\infty} \sum_{n=1}^{\infty} A(n) \left(1 - \frac{T_2}{T_1}\right)^n \frac{e^{-\frac{\omega^2}{4nc}}}{\sqrt{nc}} \cos(\omega z) d\omega \\
 &= \frac{2\sqrt{T_2}}{\pi} x_f \int_0^{\infty} \text{sinc}(\omega x_f) \cos(\omega z) d\omega - \frac{2\sqrt{T_2}}{T_2} x_f \int_0^{\omega_1} \text{sinc} \omega x_f \cos(\omega z) d\omega \\
 &\quad - \frac{\sqrt{T_2}}{\sqrt{\pi}} \sum_{n=1}^{\infty} A(n) \left(1 - \frac{T_1}{T_2}\right)^n \frac{1}{\sqrt{nc}} \left[\int_0^{\infty} e^{-\frac{\omega^2}{4nc}} \cos(\omega z) d\omega - \int_0^{\omega_1} e^{-\frac{\omega^2}{4nc}} \cos(\omega z) d\omega \right]
 \end{aligned}$$

Applying the Trigonometric identity

$$\sin(\omega x_f) \cos(\omega z) = \frac{1}{2} \sin(x_f + z) \omega + \sin(x_f - z) \omega$$

and integrating, we get

$$\begin{aligned}
 h_1(z) &= \frac{\sqrt{T_2}}{\pi} \left[\frac{\pi}{2} + \frac{\pi}{2} \right] = \frac{\sqrt{T_2}}{\pi} \text{Si}(x_f + z) \omega_1 - \frac{T_2}{\pi} \text{Si}(x_f - z) \omega_1 \\
 &\quad - \frac{\sqrt{T_2}}{\sqrt{\pi}} \sum_{n=1}^{\infty} A(n) \left(1 - \frac{T_1}{T_2}\right)^n \frac{1}{\sqrt{nc}} \sqrt{n\pi c} e^{-cnz^2}
 \end{aligned}$$

$$+ \frac{\sqrt{T_2}}{\sqrt{\pi}} \sum_{n=1} A(n) \left(1 - \frac{T_1}{T_2}\right)^m \frac{1}{\sqrt{nc}} \int_0^1 e^{-\frac{\omega^2}{4nc}} \cos(\omega z) d\omega$$

Finally, the pulse image is given by

$$h_1(z) = \sqrt{T_2} - \frac{\sqrt{T_2}}{\pi} \left[\text{Si}(x_f + z) \omega_1 + \text{Si}(x_f - z) \omega_1 \right] \\ - \sqrt{T_2} \sum_{n=1} A_n \left(1 - \frac{T_1}{T_2}\right)^n e^{-cnz^2} \\ + \frac{\sqrt{T_2}}{\sqrt{\pi}} \sum_{n=1} A(n) \left(1 - \frac{T_1}{T_2}\right)^n \frac{1}{\sqrt{nc}} \int_0^1 e^{-\frac{\omega^2}{4nc}} \cos(\omega z) d\omega$$

Rewriting the image term in the following form where

$$a = \frac{\omega_1}{\sqrt{2c}}, \quad m = z\sqrt{2c}, \quad \frac{\omega}{\omega_1} = t, \quad \text{and} \quad d\omega = \omega_1 dt$$

$$h_1(a, m) = \sqrt{T_2} - \frac{\sqrt{T_2}}{\pi} \left[\text{Si}(x_f \sqrt{2c} + m) a + \text{Si}(x_f \sqrt{2c} - m) a \right] \\ - \sqrt{T_2} \sum_{n=1} A(n) \left(1 - \frac{T_1}{T_2}\right)^n e^{-\frac{nm^2}{2}} \\ + \frac{\sqrt{T_1}}{\sqrt{\pi}} \sum_{n=1} A(n) \left(1 - \frac{T_1}{T_2}\right)^n \frac{a}{\sqrt{2n}} \int_{-1}^1 e^{-\frac{a^2 t^2}{2n}} \cos(amt) dt$$

Since c , the pulse variance is large, then $x_f \sqrt{2c}$ is large and the value of $\text{Si}(x_f \sqrt{2c} \pm m) a$ approaches $\pi/2$. Under this condition, the image reduces to

$$h_1(a, m) = -\sqrt{T_2} \sum_{n=1} A(n) \left(1 - \frac{T_1}{T_2}\right)^n e^{-\frac{nm^2}{2}}$$

$$+ \frac{\sqrt{T_2}}{\sqrt{\pi}} \sum_{n=1}^{\infty} A_n \left(1 - \frac{T_1}{T_2} \right)^n \frac{a}{\sqrt{2n}} \int_{-1}^1 e^{-\frac{a^2 t^2}{2n}} \cos(amt) dt$$

At this point, it is necessary to compute the values of the integral

$$\frac{a}{\sqrt{2\pi n}} \int_{-1}^1 e^{-\frac{a^2 t^2}{2n}} \cos(amt) dt$$

Upon receiving these values, it is then possible to normalize the total energy of the filtered cases to the unfiltered case.

The cases computed were those where "a" had the values of 1/4, 1/2, 1 and 2 and n varied from 1 to 5. m was taken in steps of .05 from 0 to 3.0. T_1 was taken in steps of .01 from 0 to .99. T_2 was set at 1.0.

The normalization procedure is the following

$$\int_{-\infty}^{\infty} \frac{h^2(a, m)}{T_2} = I(a, m)$$

which is normalized to the total energy of the unfiltered pulse

$A_p = I(0, m)$ where $a = 0$. Therefore, the normalization factor is

$$N = \frac{A_p}{I(a, m)}$$

The area of the filtered image, $I(a, m)$ is approximated by Simpson's rule for normalization purposes.

Representative results of the computations were plotted (Fig. 4 a through h).

The parameters relating "k", the linear frequency, and "c", the pulse variance for "a's" varying from 0 to 2 are plotted in Fig. 5. This relationship is defined by

$$c = \frac{2\pi^2 k^2}{a^2}$$

For the entire range of edge contrast (Variation of T_1), the smaller filter sizes give the expected results: increased normalized contrast for increased filter size. The larger filter sizes give rather unexpected and varying results for changing contrast. A full explanation for this phenomenon cannot be made without further study.

Experimental Filtering of a Non-Sharp Edge

In order to substantiate the theoretical work, an experiment was designed with conditions approximating the analysis.

Instead of a pulse, a filmed non-sharp edge was used as an object, being placed in the object plane of the Image Enhancement Viewer. Though this pulse had first been assumed to be of Gaussian shape, subsequent traces have revealed a number of "unGaussian" characteristics which could well affect the resulting filtered traces.

Because an edge was used, and not a pulse, the filters placed in the object plane did not have to be circular (the frequency distribution being one dimensional. The occluding filters used were pieces of drill rod whose width was accurately known. These filters were then carefully centered in the frequency (or filter) plane.

Using a scanning photometer whose slit width was minimized to the point where, at maximum photometer sensitivity, using the largest filter, 100% deflection on the recorder (5 mv range) could be reached. The edge was then traced with the photometer placed in the image plane with its slit parallel with the edge. First, the image of the edge with no occluding filter and the images of the edge with filters corresponding to $a = 1.5$ and $a = 2.5$ were traced.

The actual traces for the three cases are found in figure 6. (The two filtered cases are expanded by a factor of ten in the intensity scale:

The resulting filtered cases were normalized to the area under the unfiltered curve in the same manner as used in the theoretical traces. The resulting curves are plotted in figure 7. Because the normalized cases are meant to be compared with the theoretical Gaussian, only the part of the edge corresponding to a pulse (center $\frac{1}{\sqrt{2}c}$ distance from the inflection point) is taken.

Because of differences between the experimental edge and the Gaussian pulse taken in Part I, and the limitations in filter size (it was not possible to obtain smaller filters), no conclusion may be drawn from the results, through a general agreement may be found.

Edge Enhancement Through Exposure Addition

The next area to be investigated was that of actually applying filtering techniques in order to "enhance" an edge on a photographic emulsion. This edge may be enhanced in two different ways; increase in contrast and/or increase in slope.

At present, two methods for producing such enhancement using the Image Enhancement Viewer have been considered. The first is called exposure addition. In this method, an unfiltered edge is exposed on an emulsion, after which an occluding filter is placed in the system and without changing the position of either the edge or the film, a second exposure is made on the same frame. The second method is transmission multiplication. Here, two exposures are made on two separate frames; one exposure is unfiltered, the other, filtered to some degree. These two frames are then combined, using some sort of enlarging technique, in various proportions. Obviously, the difficulty in this method is the alignment of the two negatives which is quite critical. This must be done with an accuracy that would entail a great deal of technical ability.

It was possible to do some work in the area of exposure addition, using the test edges from the previous area, but because of time limitation, it was impossible to do any transmission multiplication.

The edge was exposed, using several occluding filters with varying exposure times, mixing the filtered and unfiltered parts. These edges were then microdensitometered on our Intectron instrument. For these traces, an effective 3 micron slit was used. The results of these traces have been recorded in Table #1.

Tables #1 and #2 refers to exposures #1-19. The slopes (Table #1) and edge contrasts (Table #2) are those read, averaged and weighted from several microdensitometer traces, varied for relative slit position with the edge. Included is the sensitometric curve relevant for the longer exposure times. Given also are the exposure times and the maximum densities (upper point through which the slope passes). As can be seen, some of these values are well up on the shoulder of the sensitometric curve (Table #3). All of the exposures were on Pan-X 70mm film. A plot of the measured edge slopes against the ratio of filtered to unfiltered exposure time is plotted in figure 8.

From this data, it may be concluded that, with correct mixtures of filtered and unfiltered exposures, it is possible to equal, or even surpass, slightly, the slope of the original edge.

Application of Spatial Filtering to the Examination of Aerial Photographs

As part of the studies with the Image Enhancement Viewer, it was considered desirable to examine some aerial negatives with various degrees of spatial filtering. The reason for this was that it is sometimes thought that details below the limit of detection can be brought above this threshold by suitable filtering. Also, it is conceivable that recognition of poorly defined objects might be improved by a controlled filtering which caused ringing at the edges.

When the detail to be detected has a well-defined spectrum, or a known pattern, spatial filtering has definite advantages. For example, a sinusoidal frequency of low modulation, recorded photographically, may be invisible against a grainy background, but by use of a spatial filter permitting only that frequency to pass, the grain "noise" is eliminated from the reconstituted image and the sinusoidal pattern may be seen. To be more precise, only those components of the grain frequency spectrum which lie in the passband of the filter remain to obscure the wanted image, and if the grain spectrum is flat this gives a great improvement in signal-to-noise ratio. However, this is an ideal case for the use of filtering, since the signal spectrum is concentrated at one point in the diffraction plane while the noise spectrum is widely distributed across the plane. When the object is more complex, for example, a square wave instead of a sine wave, its spectrum theoretically extends to infinity, and noise cannot be reduced without distorting the signal in some degree. If the significant feature of the object, however, is its repetitive nature and not the shape of the waves, the filtering can be as effective as for the sinusoidal pattern. For aerial scenes in general, little or no improvement can be expected from spatial filtering, because the details, consisting of sharp edged lines

or similar simple non-repetitive shapes, have very complex spectra. Filtering to reduce noise can only be effective if the objects of interest have simple known spectra, for which individual filters can be made in advance.

To test these ideas under a realistic approximation to practical conditions, the following experimentation was carried out, with a set-up which was being used in another program. Simulated aerial photographs were made by photographing a transparency made under controlled tone-reproduction conditions from a large-scale aerial negative. The original negative scale was 1:2000 and the reduction factor, using a 6 inch lens, was 20 to 1, thus the copy negative were at 1:40,000 scale. Uniform fogging light from a beam-splitter was introduced during the copying, to reduce the luminance scale of the transparency to approximately 5 to 1, simulating an aerial scene viewed from a high altitude. Negatives were made on SO 243 emulsion, varying the lens/film transfer function by changing the lens aperture. These lens/film transfer functions are shown in figure 9; for these values of spatial frequency cut-off, granularity is not obtrusive when looking for detail in the negatives. Thus a series of negatives were available in which the quality of definition showed a progressive deterioration of known amount. The intention was to apply various kinds of filtering, and if any improvement could be seen, to equate this to the quality of the next best negative. Thus any effect of the filtering could be approximately evaluated in terms of the definition of conventionally-viewed photographs.

The original 1:40,000 scale negatives, being only 1 cm in diameter, were enlarged X6, the resulting positive transparencies being more convenient for viewing in the spatial-filtering apparatus. (It was known, from work in the other programs referred to above, that the enlarging process introduced no significant loss of quality even for the best negative.)

After repeated trials of filtering, both high-pass & low-pass, it was concluded that no choice of frequency band enabled anything to be seen which could not be seen as well or better in normal viewing by incoherent light. Indeed, due to the disturbing effect of the ringing around small particles of dirt which had not been completely removed from the negatives or filtered from the fluid, the incoherent viewing was always preferred. In a few instances it was felt that the edges of isolated objects such as trucks might have been more clearly defined when using a high-pass filter, but this effect was so small, (if it existed) that a follow-up with more precise experimentation was not justified.

This negative conclusion is in accordance with the theoretical expectations, as discussed earlier in this section.

It should perhaps be stressed that these findings do not imply that coherent light techniques have no value for the detection of previously-known patterns.

25X1B

Next 2 Page(s) In Document Exempt

CHARACTERISTICS OF TRACED ENHANCED EDGES

Table #1

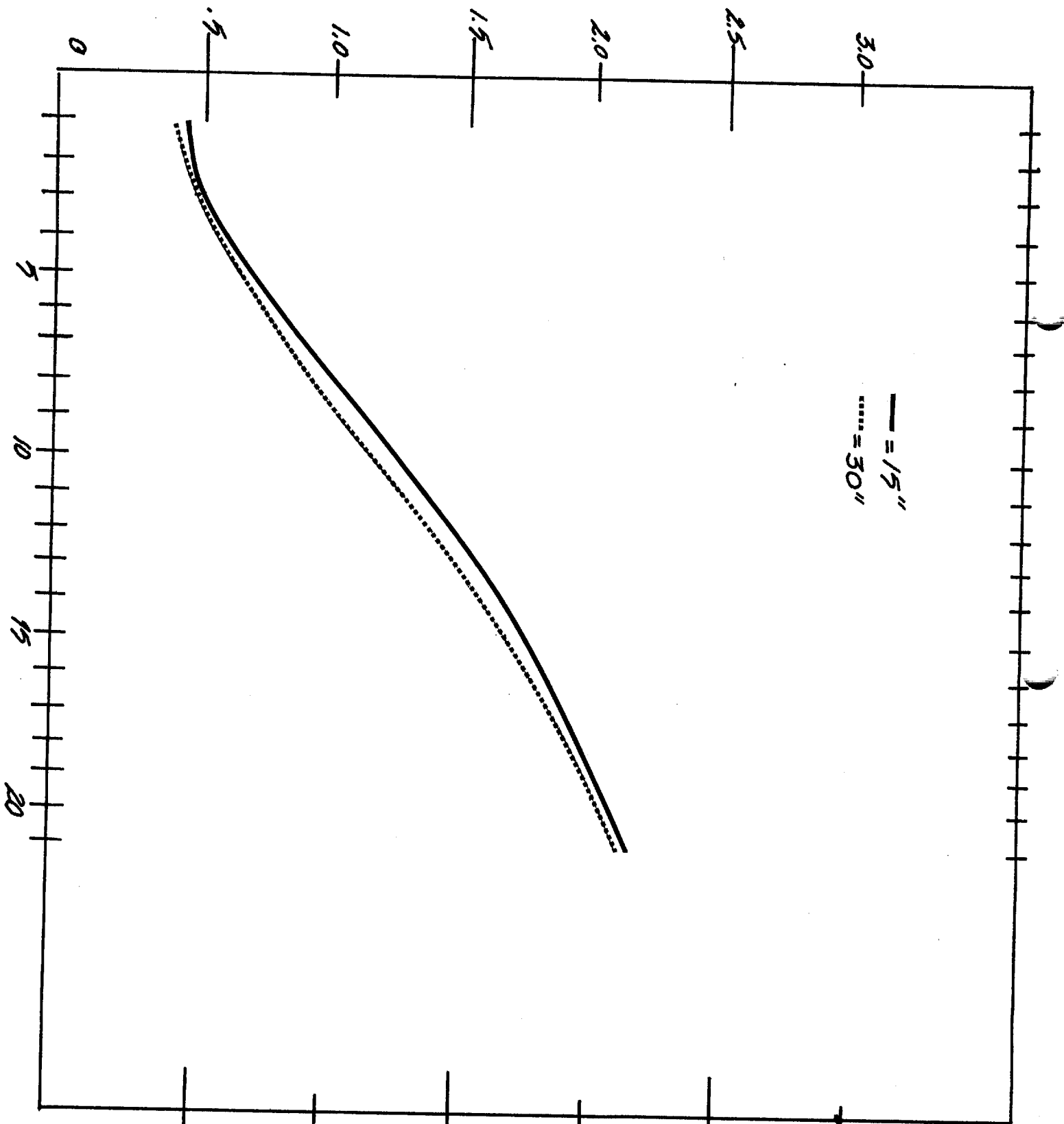
<u>Exposure No.</u>	<u>Filter (IN)</u>	<u>Average Slope</u>	<u>Unfiltered Time</u>	<u>Filtered Time</u>
1	-	4.5	1/2	-
2	-	3.5	1	-
3	.015	3.2	1/2	1
4	.015	2.5	1/2	2
5	.015	3.6	1/2	4
6	.015	4.3	1	1
7	.015	2.8	1	2
8	.015	2.4	1	4
9	.025	2.8	1/2	2
10	.025	4.0	1/2	4
11	.025	4.1	1/2	8
12	.025	2.8	1	4
13	.025	2.9	1	8
14	.041	2.8	1/2	4
15	.041	3.1	1/2	8
16	.041	5.0	1/2	16
17	.041	3.2	1	4
18	.041	2.0	1	8
19	.041	1.9	1	16

Table #2

<u>Exposure #</u>	<u>Min.</u>	<u>Max.</u>	<u>Contrast</u>
1	.60	1.50	.90
2	.95	1.20	.85
3	.85	1.45	.60
4	1.35	1.80	.45
5	1.55	1.90	.35
6	1.15	1.85	.70
7	1.50	2.00	.50
8	1.40	1.90	.50
9	.80	1.55	.75
10	1.20	1.70	.50
11	1.00	1.60	.60
12	1.10	1.80	.70
13	1.35	1.85	.50
14	.85	1.55	.70
15	.75	1.50	.75
16	.90	1.55	.65
17	.95	1.70	.75
18	1.30	1.80	.50
19	1.65	2.25	.60

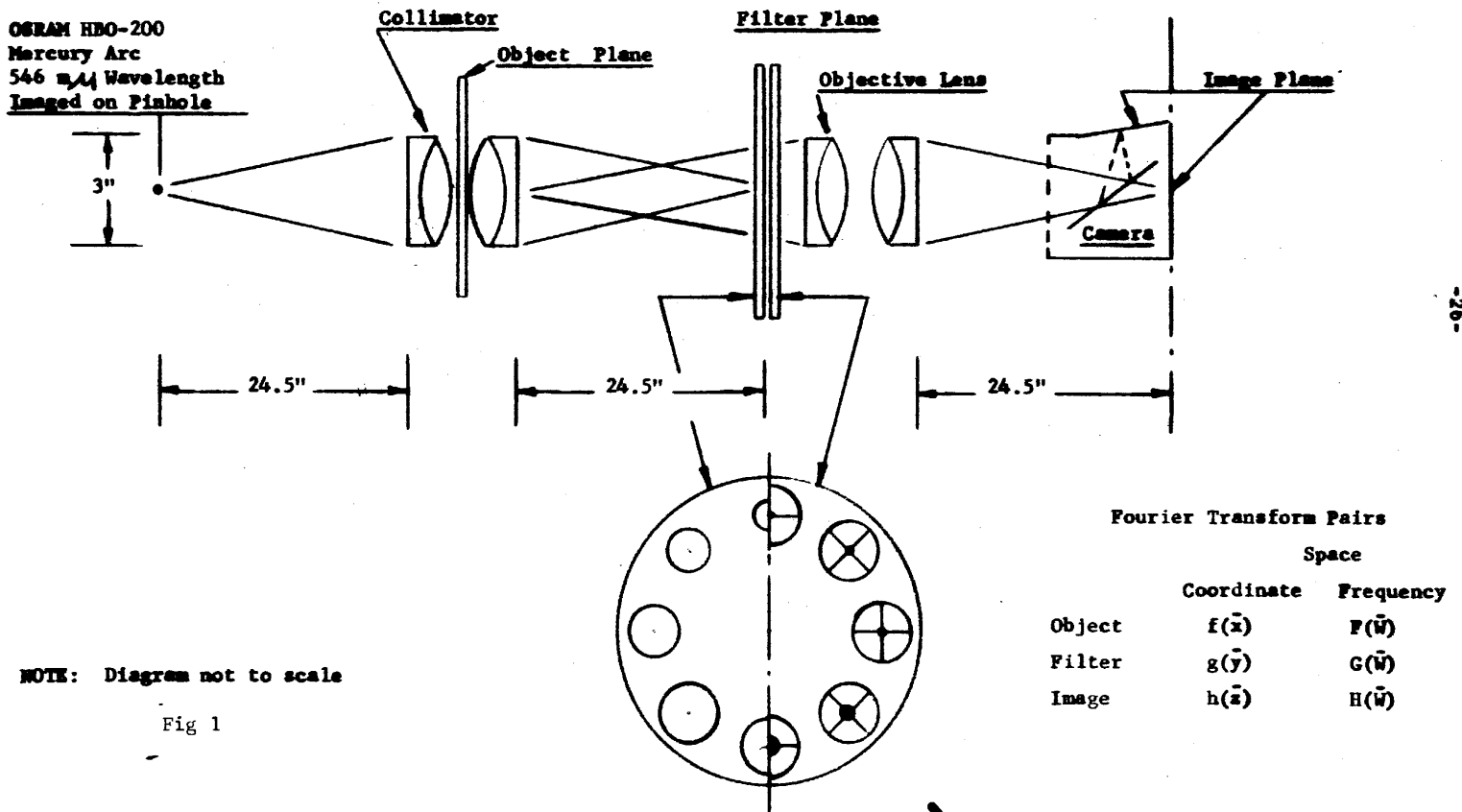
*SENSITOMETRIC CURVES FOR
ENHANCED EDGES
PANATOMIC-X, D-19 6 MIN.*

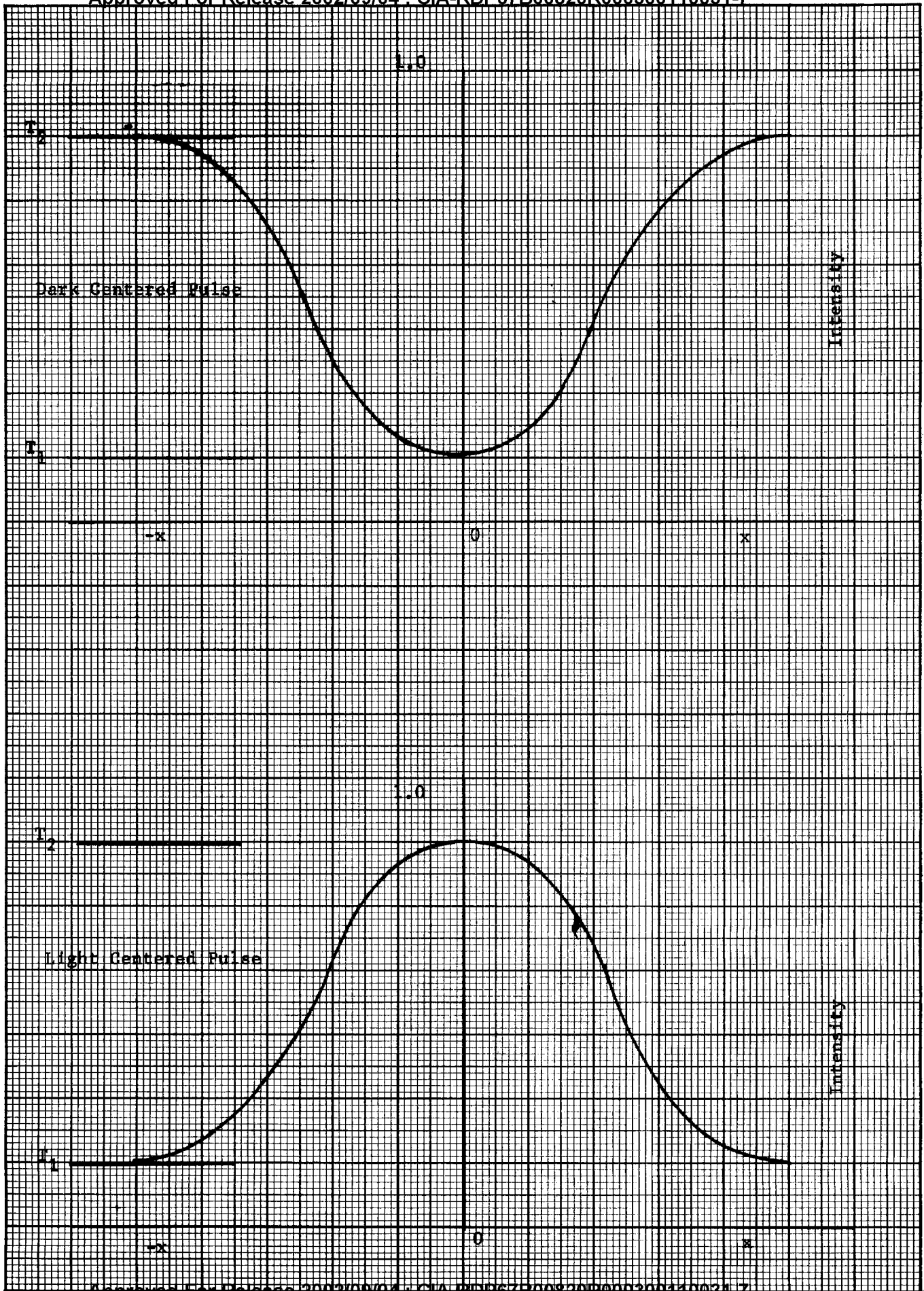
TABLE #3



Major Features and Dimensions of
Image Enhancement Viewer

(Approximate overall system length = 8 feet)





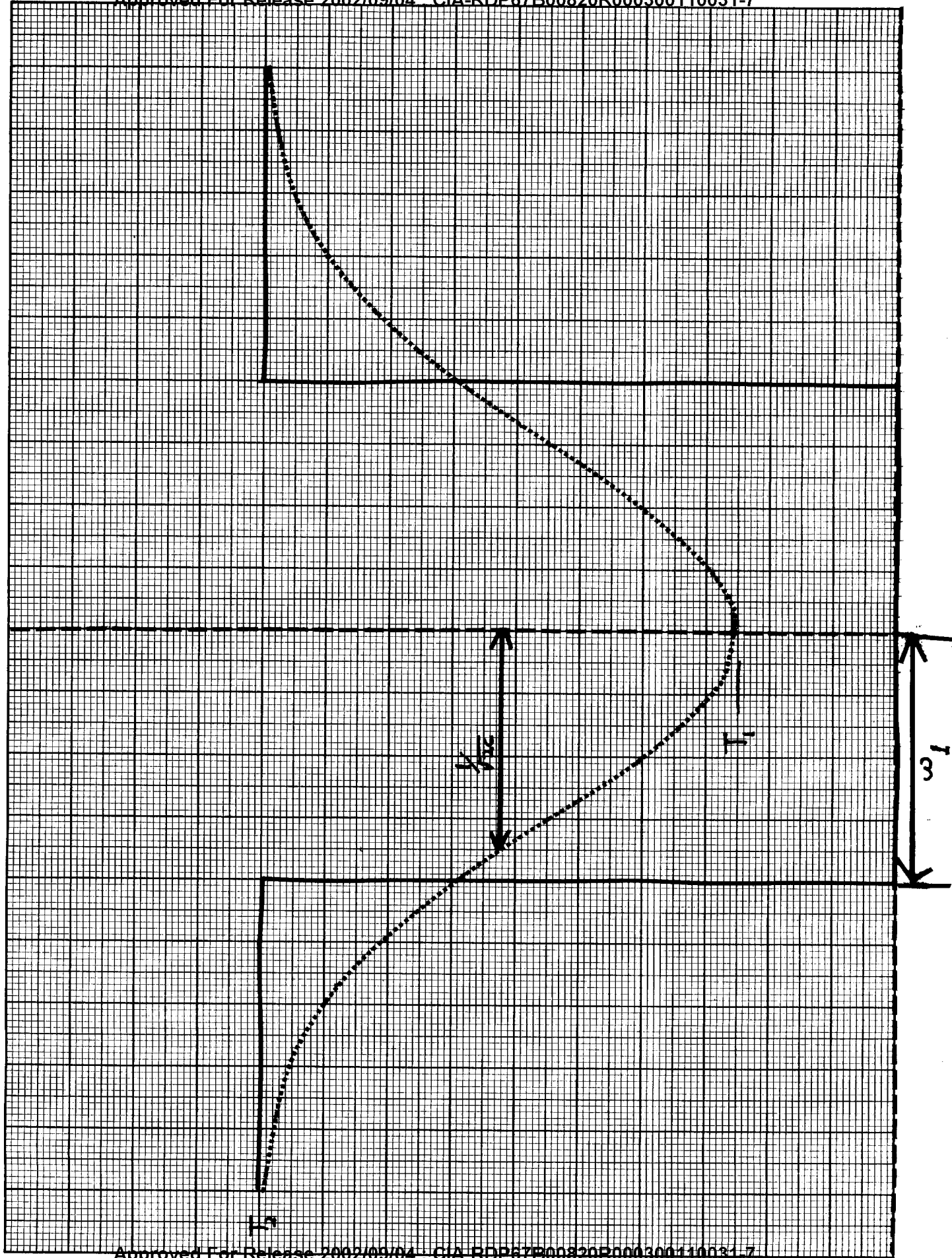


Fig. 3

K-E 10 X 10 TO 1/2 INCH 46 1323
7 X 10 INCHES
KEUFFEL & ESSER
MADE IN U.S.A.

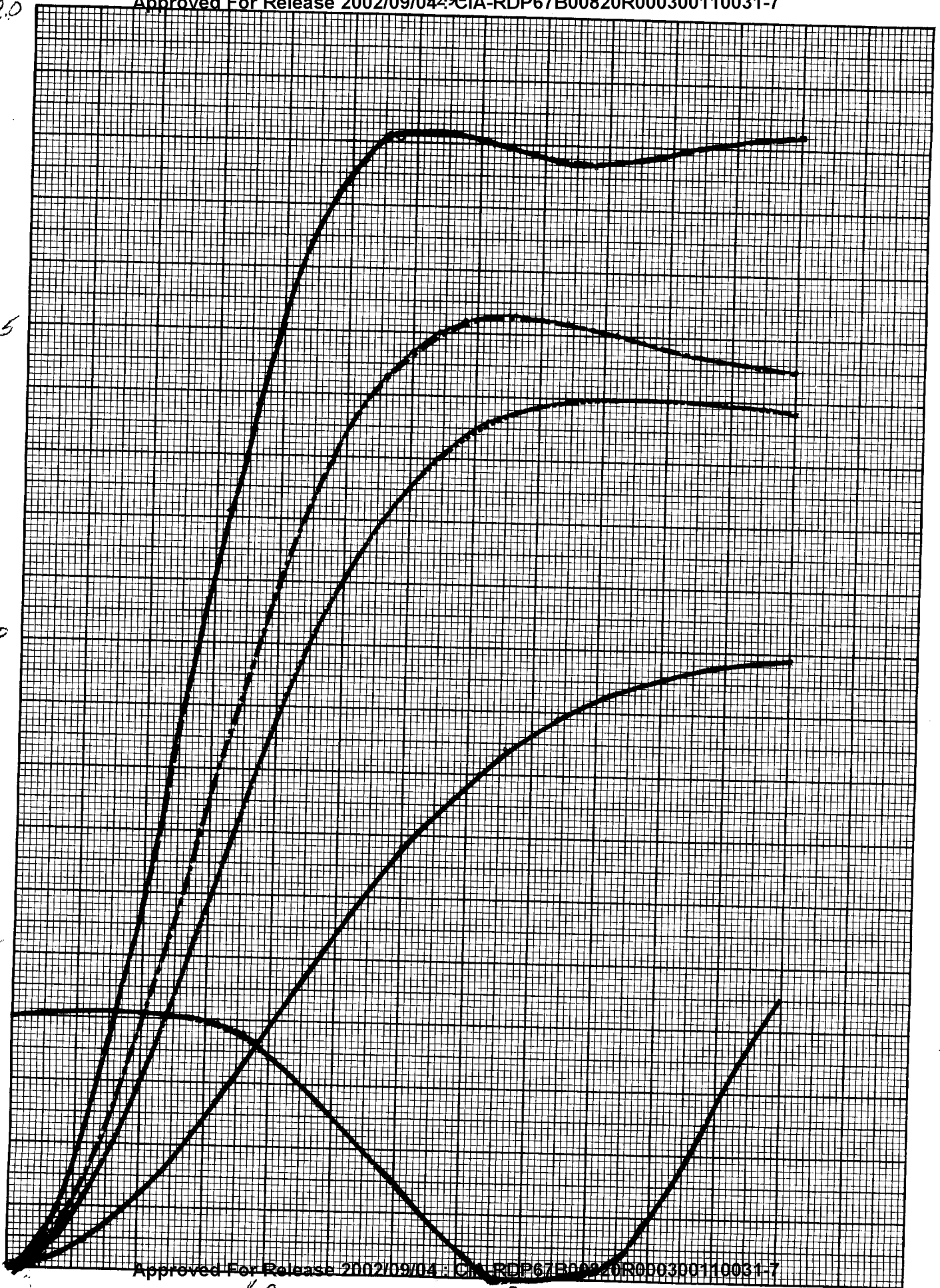
GAUSSIAN SPATIAL PULSE WITH OCCLUDING SPATIAL FILTER

K-E 10 X 10 TO 1/2 INCH
7 X 10 INCHES
KEUFFEL & ESSER
46 1323
MADE IN U.S.A.

NORMALIZED IMAGE INTENSITY

Approved For Release 2002/09/04 : CIA-RDP67B00820R000300110031-7

$T_1 = 0$



Approved For Release 2002/09/04 : CIA-RDP67B00820R000300110031-7

Fig 4a

$T_1 = .1$

K&E 10 X 10 TO 1/2 INCH 46 1323
7 X 10 INCHES
KEUFFEL & ESSENE CO. MADE IN U.S.A.

NORMALIZED IMAGE INTENSITY

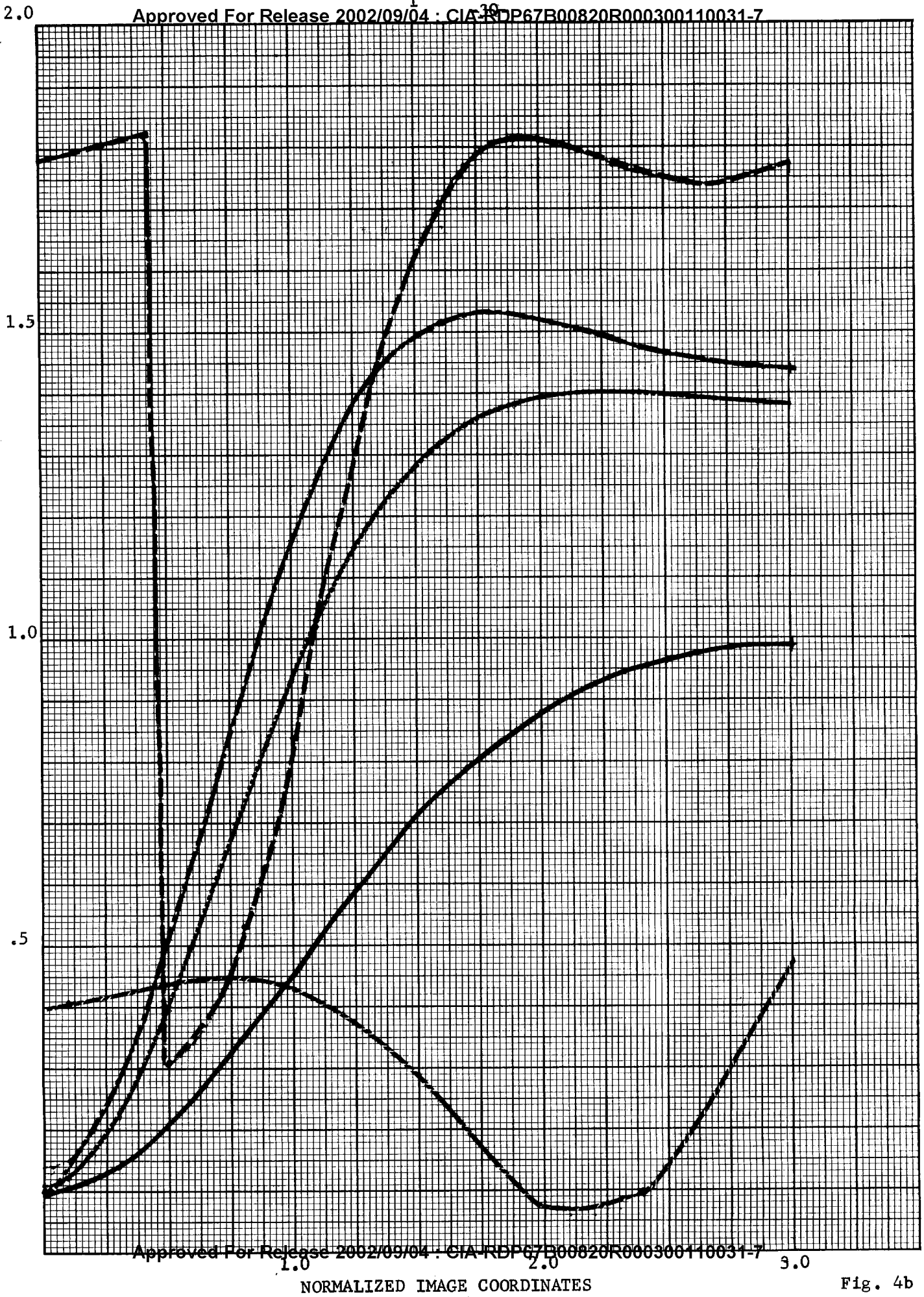


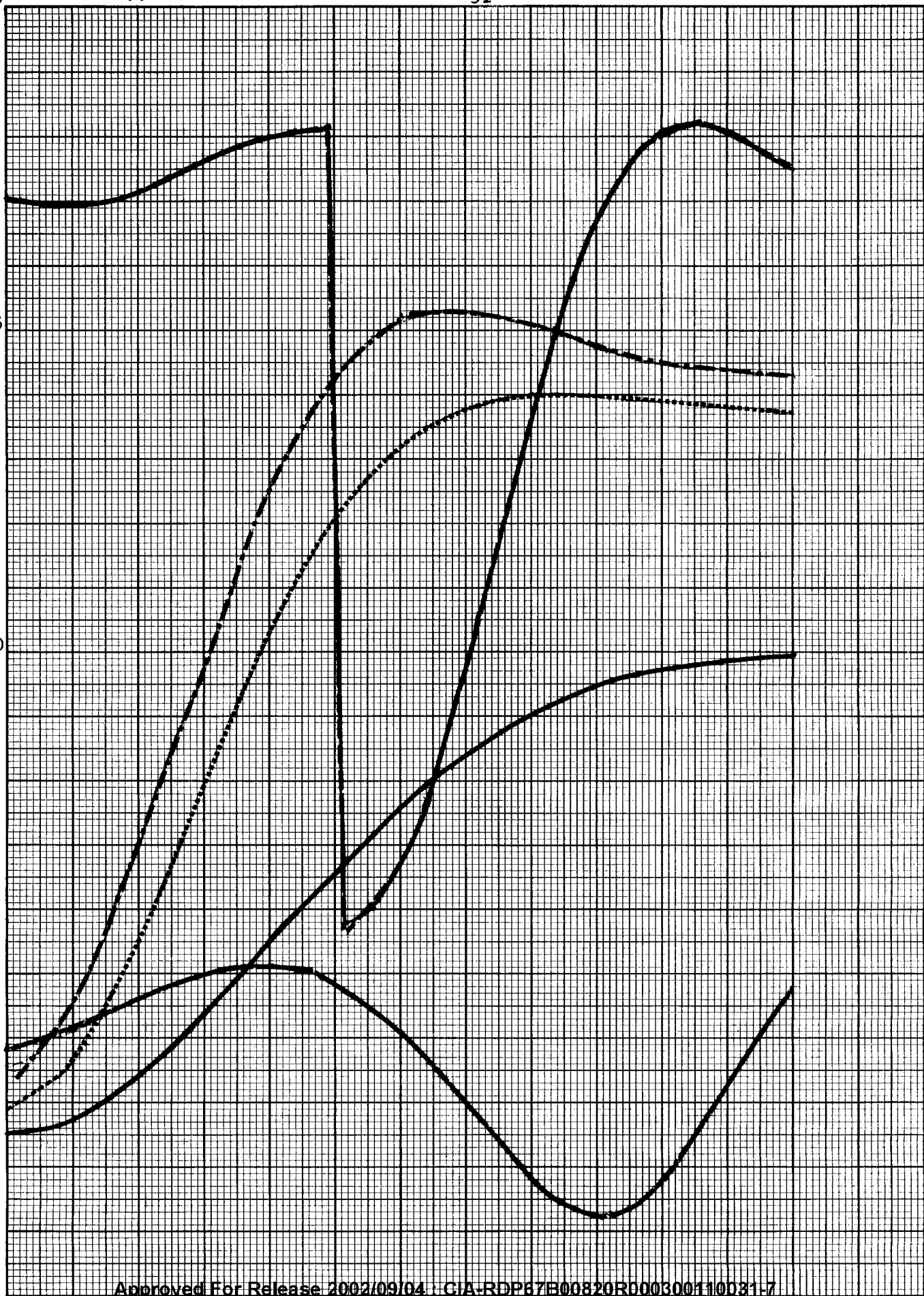
Fig. 4b

K&E 10 X 10 TO 1/2 INCH 46 1323
7 X 10 INCHES
KEUFFEL & ESSER

NORMALIZED IMAGE INTENSITY

Approved For Release 2002/09/04 : CIA-RDP67B00820R000300110031-7

$T_1 = .25$



Approved For Release 2002/09/04 : CIA-RDP67B00820R000300110031-7

NORMALIZED IMAGE COORDINATES

Fig. 4c

$T_2 = .30$

K&E 10 X 10 TO 1/2 INCH 46 1323
7 X 10 INCHES
KEUFFEL & ESSER
MADE IN U.S.A.
NORMALIZED IMAGE INTENSITY

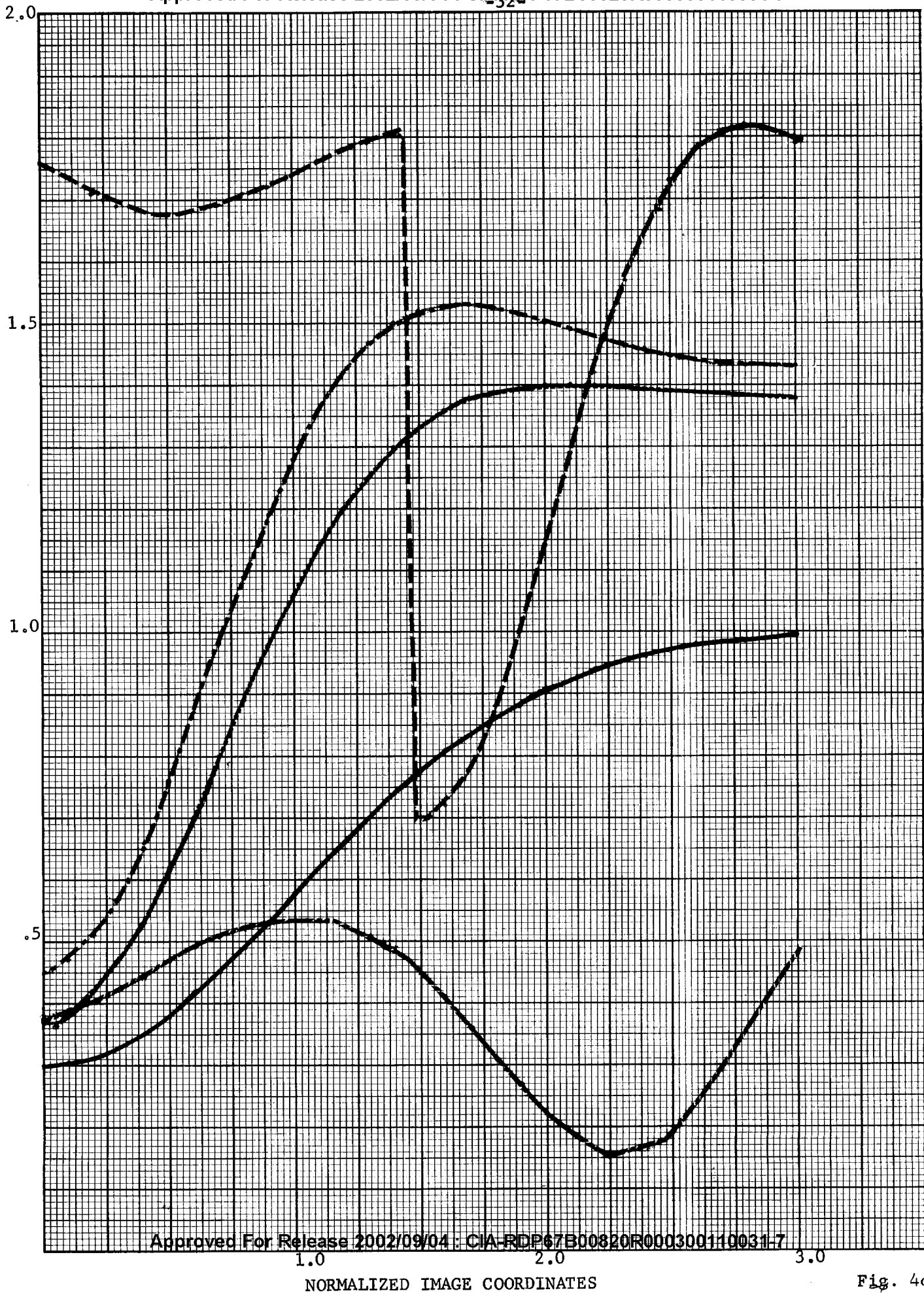
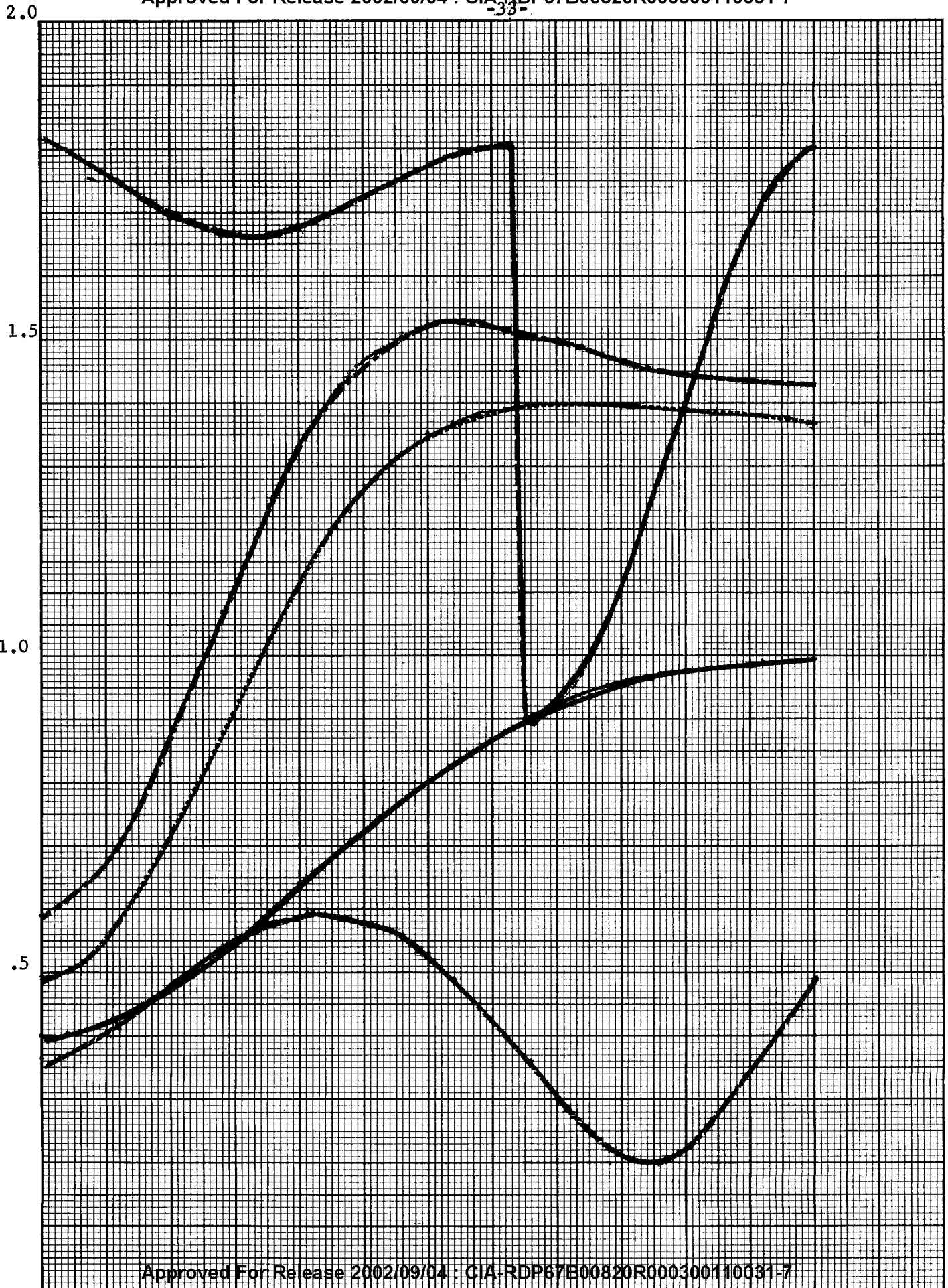


Fig. 4d

K-E 10 X 10 TO 1/2 INCH 46 1323
7 X 10 INCHES
KEUFFEL & ESSER CO. IN U.S.A.

NORMALIZED IMAGE INTENSITY



KE 10 X 10 TO 1/2 INCH 46 1323
7 X 10 INCHES
KEUFFEL & ESSER
MADE IN U.S.A.

NORMALIZED IMAGE INTENSITY

2.0

1.5

1.0

.5

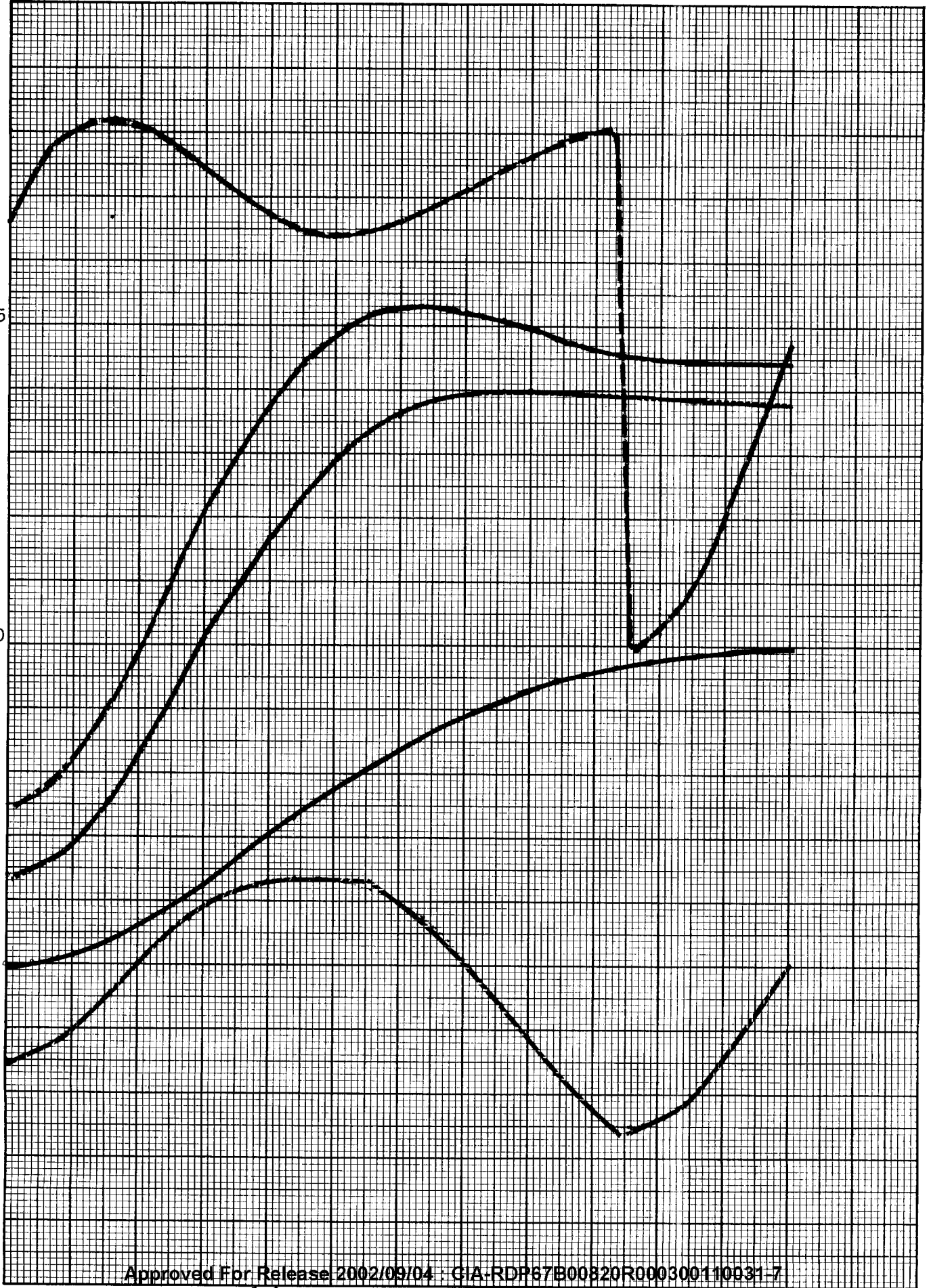
1.0

2.0

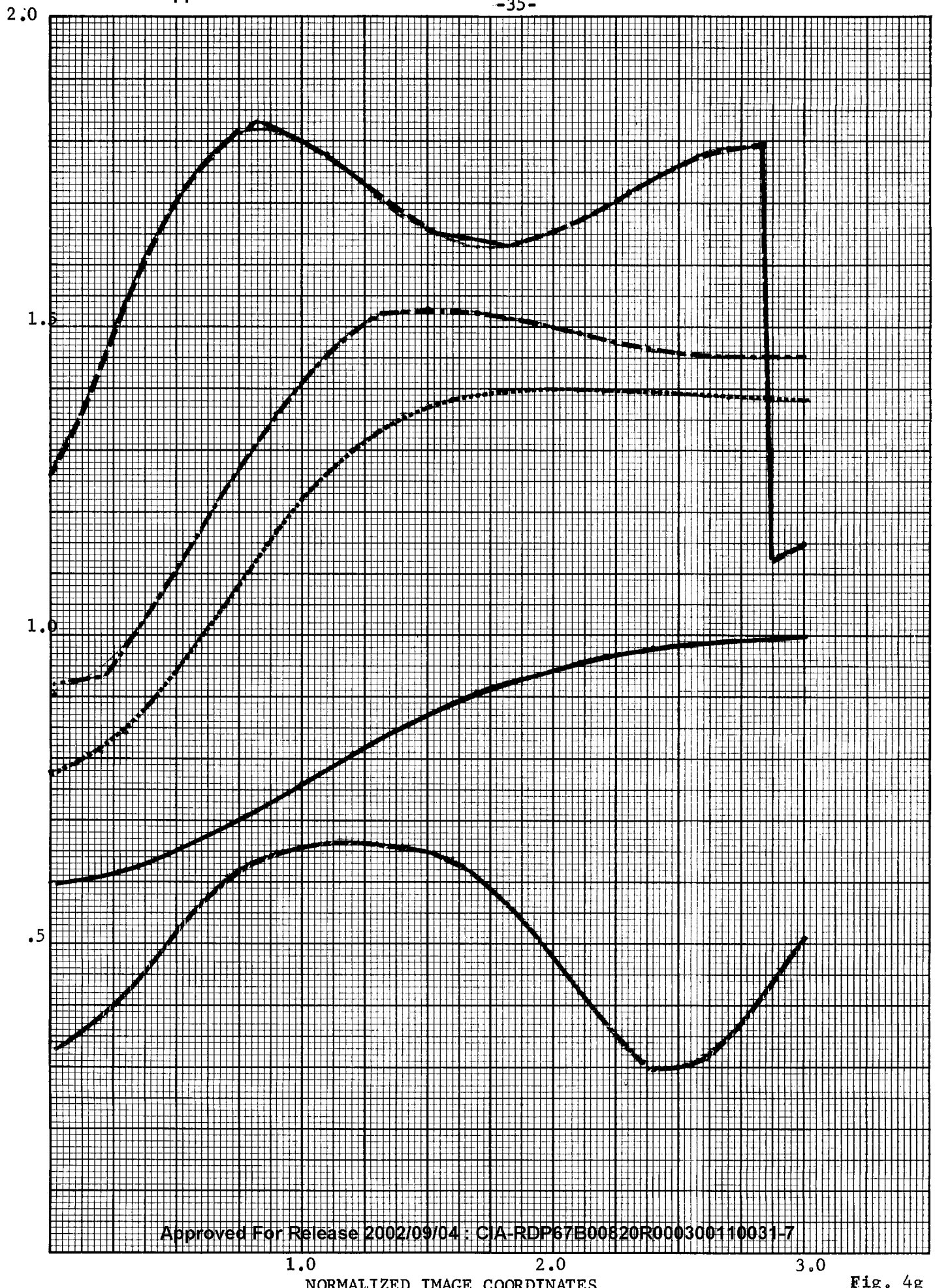
3.0

NORMALIZED IMAGE COORDINATES

Fig. 4f



K&E 10 X 10 TO 1/4 INCH 46 1323
7 X 10 INCHES
KEUFFEL & ESSER CO. U.S.A.
NORMALIZED IMAGE INTENSITY



$T_1 = .7$
-36-

2.0

1.5

1.0

.5

1.0

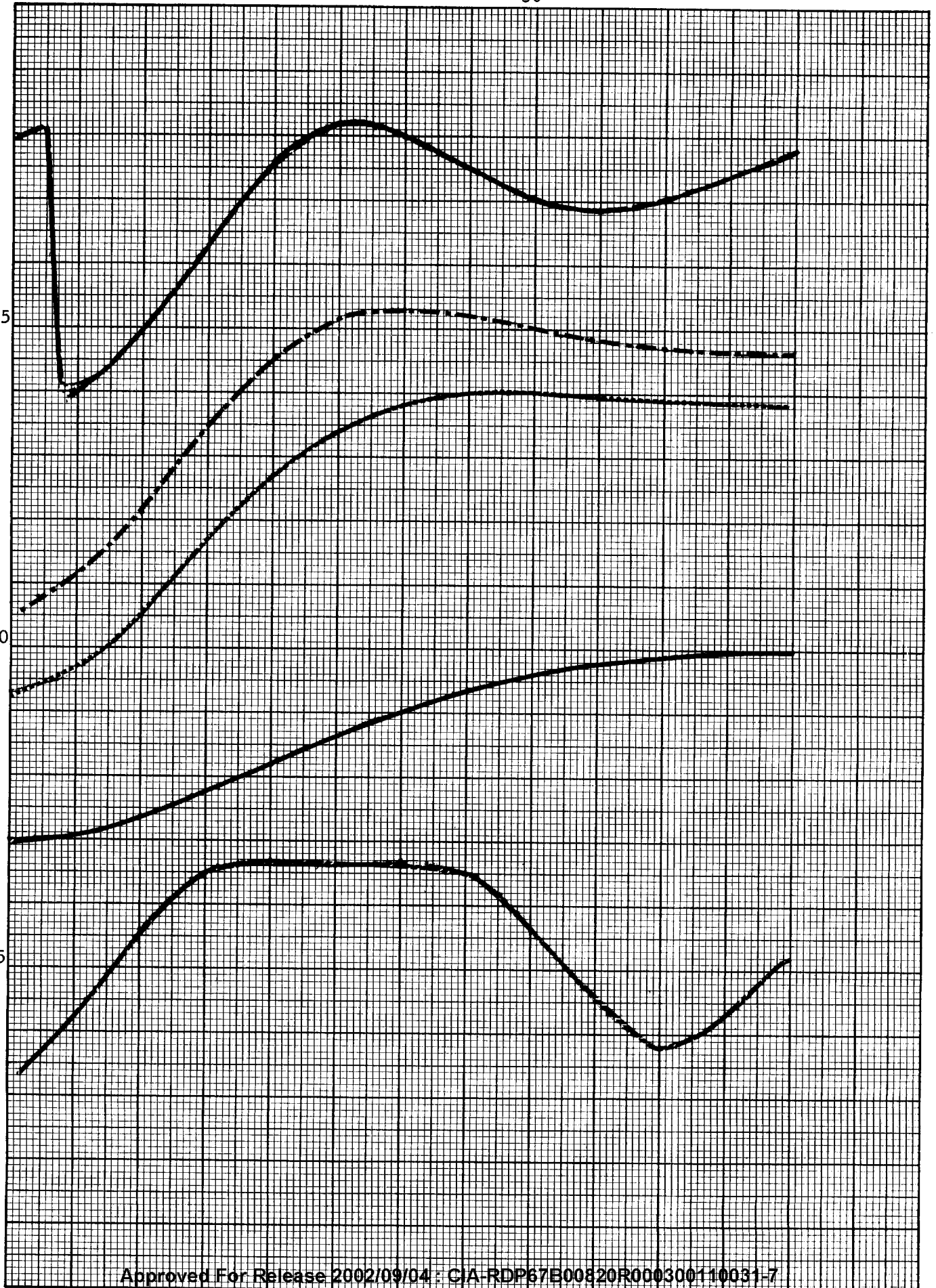
2.0

3.0

Fig 4h

NORMALIZED IMAGE INTENSITY Y

NORMALIZED IMAGE COORDINATES



FREQUENCY VS PULSE VARIANCE

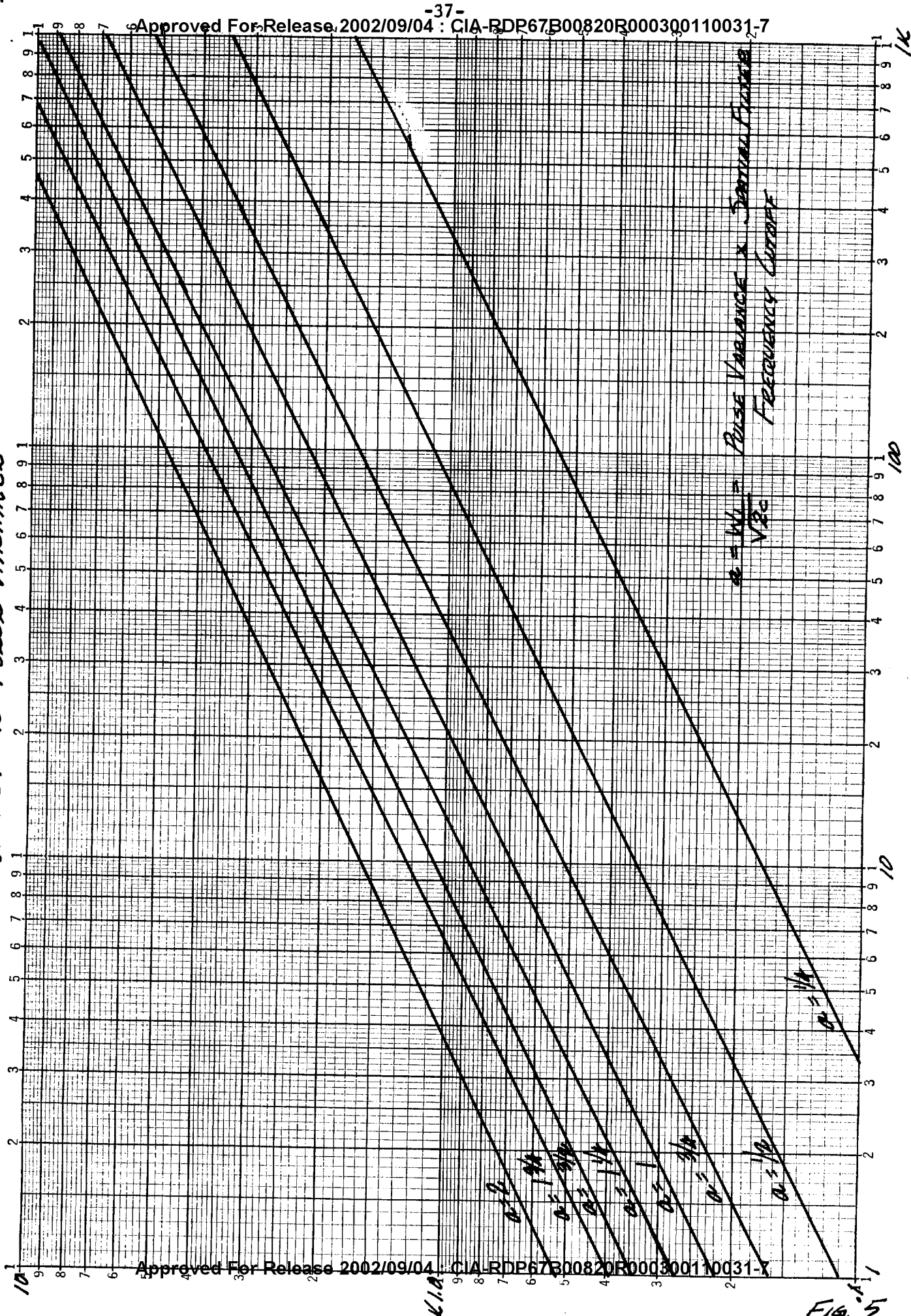


FIG. 5

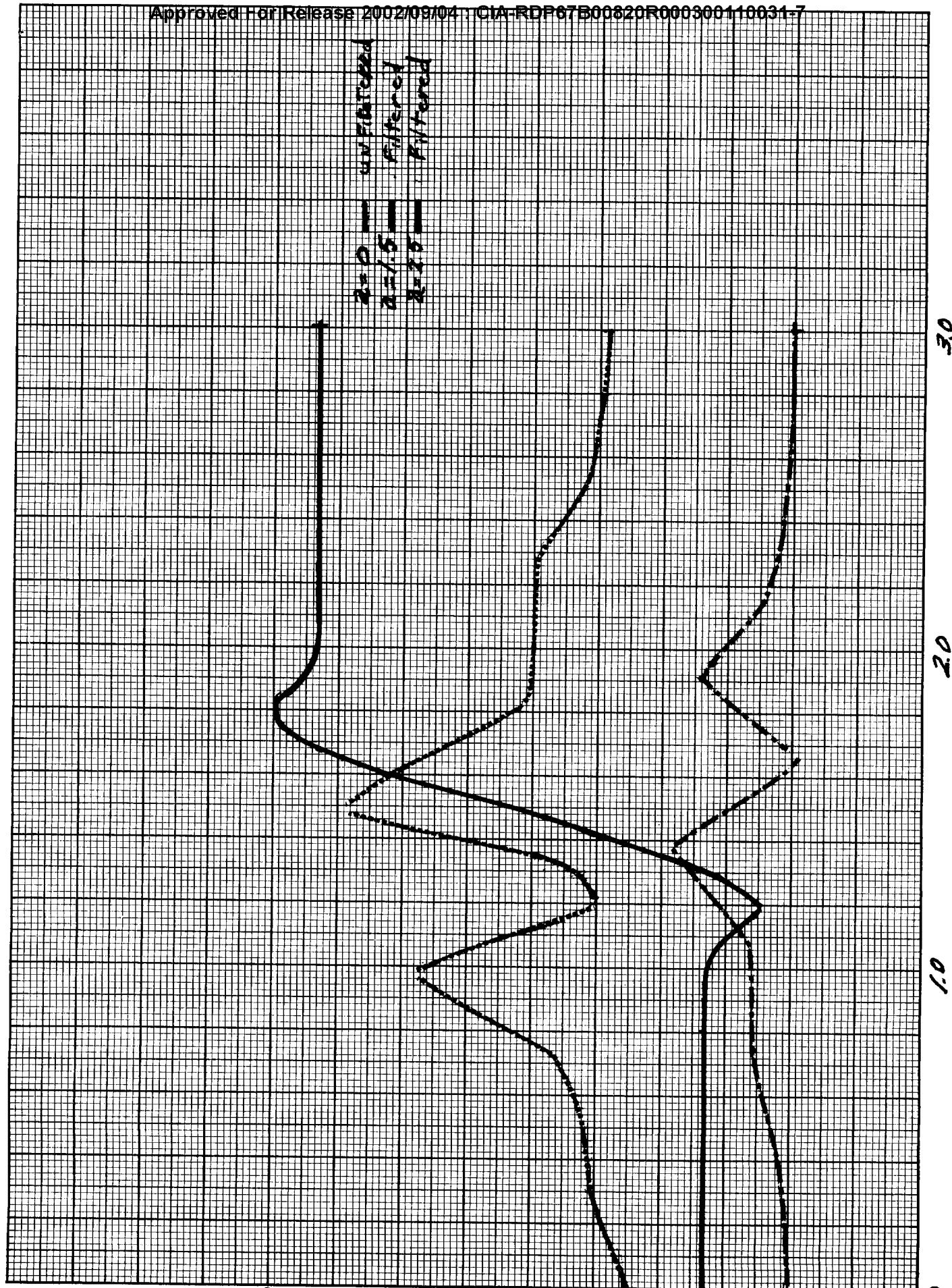


Fig 6

Normalized Image Coordinates
7 X 10 INCHES
MADE IN U.S.A.

Intensity

K&E 10 X 10 TO 1/2 INCH 46 1323
7 X 10 INCHES
MADE IN U.S.A.
KEUFFEL & ESSER

NORMALIZED IMAGE INTENSITY

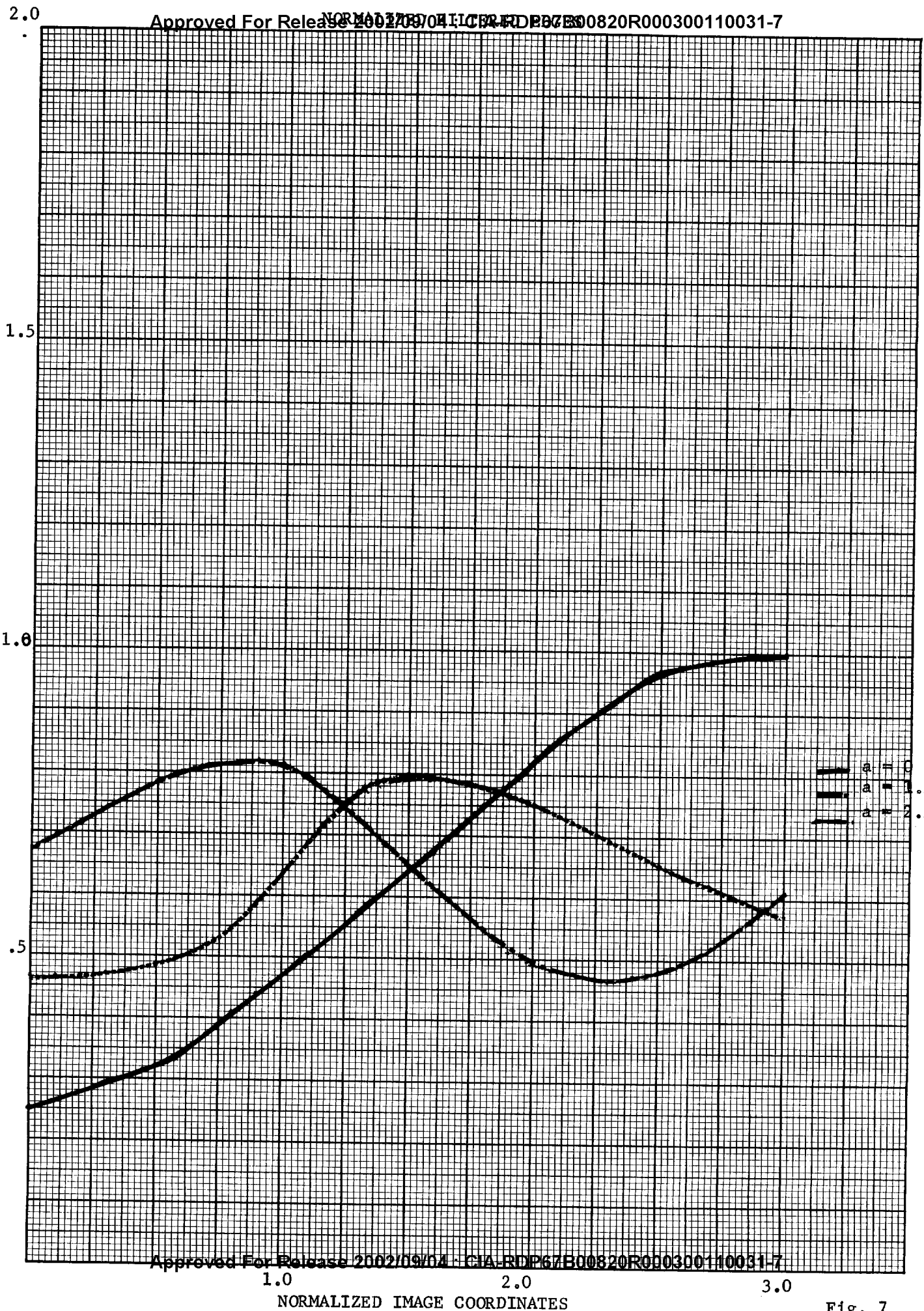
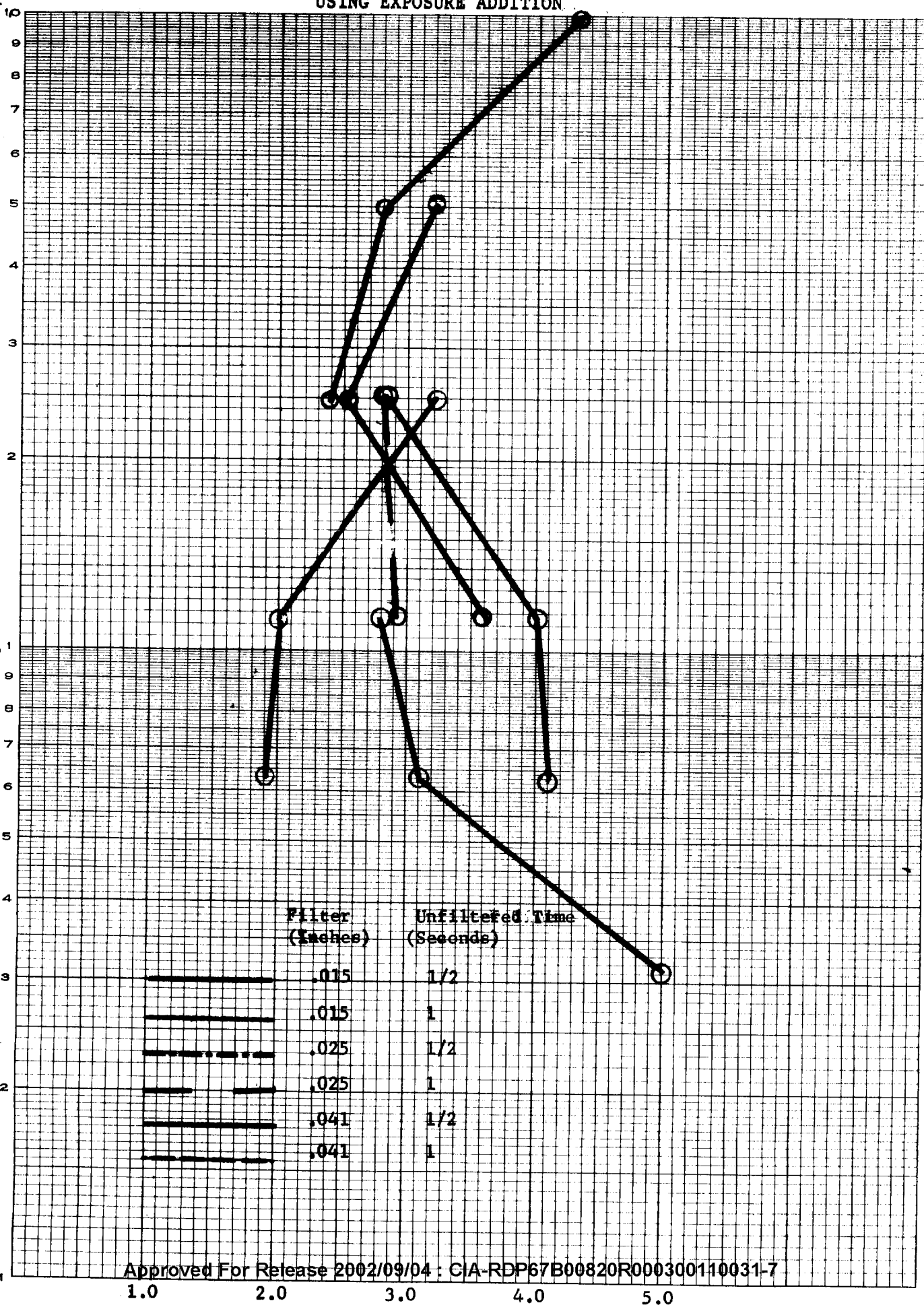
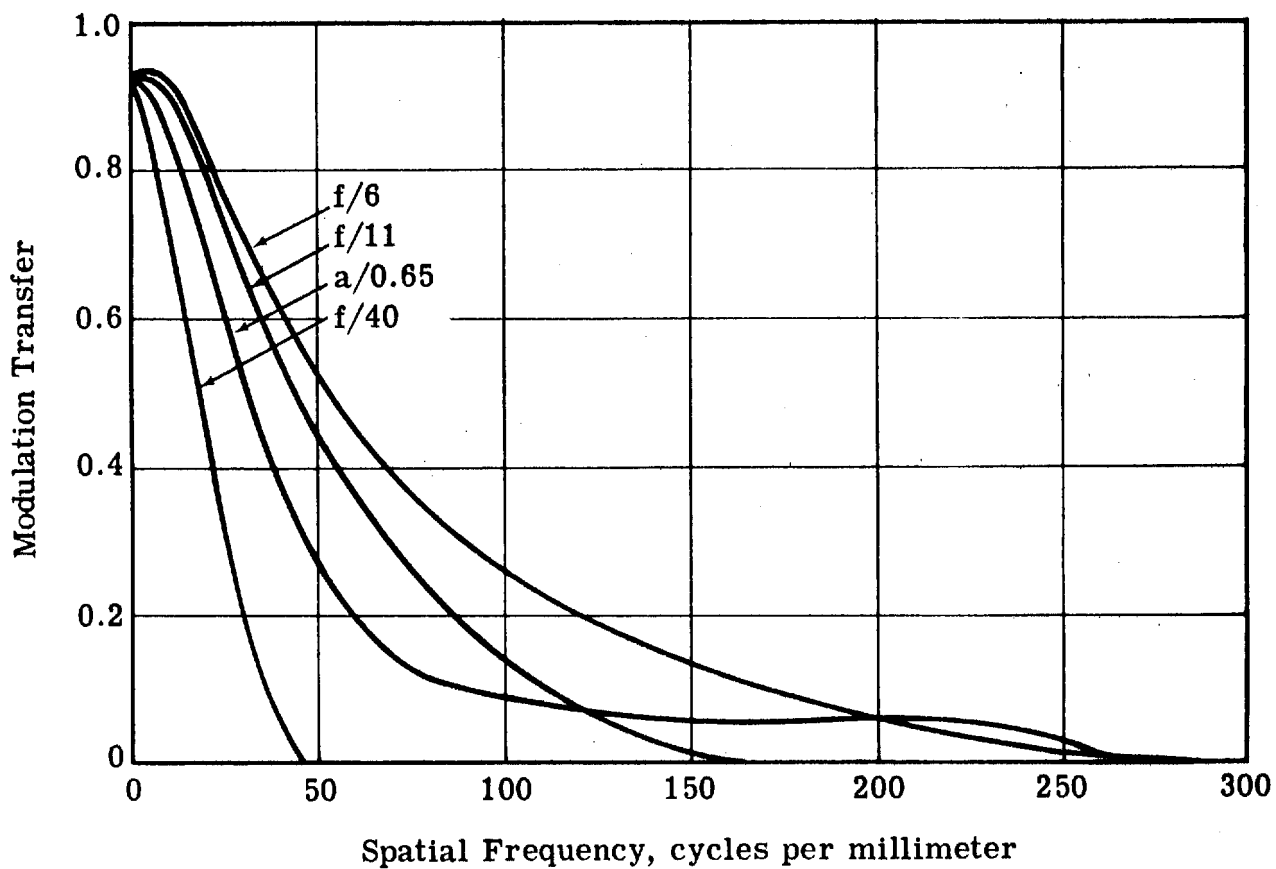


Fig. 7





Four lens-film transfer functions: SO-243

Fig. 9